# Investigations on ratcheting and post–ratcheting tensile behavior of a 7075-T6 Aluminum alloy

Thesis submitted in partial fulfillment of the requirements for the degree

of

**Master of Technology**
**in**
**Metallurgical and Materials Engineering**


Submitted By

**Lala Amarnath**

Roll No- 213MM1462




Department of Metallurgical and Materials Engineering
National Institute of Technology
Rourkela-769008


2015

# Investigations on ratcheting and post–ratcheting tensile behavior of a 7075-T6 Aluminum alloy

Thesis submitted in partial fulfillment of the requirements for the degree

of

**Master of Technology**
**in**
**Metallurgical and Materials Engineering**


Submitted By

**Lala Amarnath**

Roll No- 213MM1462

Under Supervision of

**Prof. Krishna Dutta**




Department of Metallurgical and Materials Engineering
National Institute of Technology
Rourkela-769008


2015


# National Institute of Technology, Rourkela

## *Certificate*

This is to certify that the thesis entitled, **"*Investigations on ratcheting and post–ratcheting tensile behavior of a 7075-T6 Aluminum alloy*"** submitted by **Lala Amarnath** in partial fulfillment of the requirements for the award of the degree of **Master of Technology** in **Metallurgical and Materials Engineering** at the **National Institute of Technology, Rourkela** is an authentic work carried out by him under my supervision and guidance.

To the best of my knowledge, the matter embodied in the thesis has not been submitted to any other University/ Institute for the award of any degree or diploma.

**Date:**

**Place: Rourkela**

**Prof. Krishna Dutta (Supervisor)**

**Department of Metallurgical and Materials Engineering**
**National institute of Technology,**
**Rourkela-769008**

# Acknowledgements

I would like to express my deep sense of gratitude and respect to my supervisor **Prof. Krishna Dutta**, Metallurgical and Materials Engineering Department, NIT Rourkela, for his inspiring guidance, constructive criticism and valuable suggestions throughout the research work. It would have not been possible for me to bring out this thesis without his help and constant encouragement.

I am sincerely thankful to **Prof. S. C. Mishra**, Head of department Metallurgical and Materials Engineering, NIT Rourkela, **Prof. B. B. Verma** and other faculty members of this department for their persistent support and advice during the course work.

I am very thankful to **Prof. K. K. Ray**, Professor, Metallurgical and Materials Engineering Department, IIT Kharagpur for his benevolent permission for conduction of ratcheting tests at IIT Kharagpur.

I am also highly grateful to laboratory members of Department of Metallurgical and Materials Engineering, NIT Rourkela, specially **Mr. S. Hembram, Mr. S. Pradhan and Mr. K. Tanty** for their help during execution of experiment.

I am thankful to **Mr. Srimant Kumar Mishra, Ms. R. Kreethi, Ms. Antara Bhattacharjee, Mr. Pranav Bhale, Mr. Rajneesh Pandey** and all my classmates and friends for their timely help during the course of this work.

Finally, I feel great reverence for all my family members and the Almighty, for their blessings and for being a constant source of encouragement.

Date:

**Place:** Rourkela **Lala Amarnath**

# Contents

# Abstract

In this work, it has been aimed to study the ratcheting and post–ratcheting tensile behavior of a 7075-T6 aluminum alloy at room temperature which is potentially used in aerospace, automobile components etc. where deformation caused by ratcheting cannot be ignored. The T6 heat treatment was done on as-received aluminum alloy rods. The heat treated rods were then characterized for the microstructural features using an optical microscope along with hardness measurements. The tensile tests were carried out on specimen designed as per ASTM standard E8M using universal tensile testing machine (INSTRON 1195). The fatigue specimens as per ASTM standard E606 were prepared and fatigue tests were done using ±250 kN servo hydraulic universal testing machine (Instron: 8800R). The effect of stress parameters such as mean stress and stress amplitude were investigated on the ratcheting behavior of the selected aluminum alloy. In order to study the post ratcheting tensile behavior of the investigated alloy, tensile tests were done on all ratcheted samples using INSTRON 1195. Also the fractographic studies of all post ratcheting tensile samples were done using a scanning electron microscope (SEM). Further, for qualitative analysis of the phases present in unratcheted and post ratcheted tensile specimens are subjected to X-Ray diffraction (XRD) analysis using Cu Kα radiation.

From the results of ratcheting tests for different combinations of mean stress and stress amplitudes it is observed that at constant mean stress, by increasing stress amplitude, ratcheting strain increases. Also saturation in strain accumulation takes places in the investigated material after around 10-20 cycles under all test conditions. The analyses of hysteresis loop generated during cyclic loading indicate that the material exhibits cyclic hardening in the initial fifty cycles which gets softened in further loading up to about 70-80 cycles and finally attains a steady state. From the post ratcheting tensile test it was observed that the yield strength of the material increases whereas the ultimate tensile strength decreases. The increase in ratcheting strain with stress parameters occurs due to increased deformation zone during cycling; also it can be correlated with increased remnant dislocation density. The cycling hardening followed by softening is correlated with characteristic precipitation features of the alloy.



**Keywords:** Aluminum 7075 alloy; Ratcheting; Stress amplitude; Mean stress; Fractography

# List of figures

# List of tables

# Chapter 1

# Introduction

# *Introduction*

## 1.1 Introduction

Aluminium has an expended variety of uses due to the combination of its favourable properties. The properties that make aluminium so emanate include its high strength to weight ratio, ease of formability, and high electrical and thermal conductivity. This metal has experienced increasing levels of use in recent years and has replaced materials such as wood, copper, and steel in many engineering applications. Aluminium alloys are classified in different types based on the various alloying elements that they contain. Under the supervision of the Aluminium Association (AA), major aluminium producers have developed a four-digit numerical designation to classify each of the different alloys. The first digit indicates the alloy group that contains specific main alloying elements. 1XXX series alloys are primarily aluminium with a minimum Al content of 99.0% [1]. The main alloying elements for 2XXX, 3XXX, 4XXX, 5XXX, 6XXX, and 7XXX series alloys are, respectively, copper, manganese, silicon, magnesium, both magnesium and silicon and zinc.

Modern monetary and military aircraft owe many of their advances in design and performance to the development of aluminium based alloys. The principal alloy of this study, AA7075-T6, is a high strength alloy used extensively for structural aircraft components. This heat treatable, precipitate age hardened Al-Zn-Mg-Cu alloy remains attractive for such applications primarily because of its high strength to weight ratio [2]. Its use in aerospace component like fuselage, wings etc. which always subjected to cyclic loading during both the time take-up and landing. One of the major failure mode under cyclic loading is known as fatigue. It is known that almost 90% of engineering failures occur due to fatigue [3]. Fatigue of engineering components is

therefore a serious issue and hence, lots of research efforts are directed to it. Fatigue failure of engineering components may be subdivided into two broad categories namely: (i) Low cycle fatigue (LCF): in this fatigue, number of applied cycle should be less than $10^4$ cycle ($N<10^4$ cycle) and (ii) High cycle fatigue (HCF): in this fatigue, number of applied cycle should be greater than $10^4$ or $10^5$ cycle ($N>10^4$or $10^5$ cycle). Further, low cycle fatigue is also of many types and one particular low cycle fatigue deformation is known as ratcheting.

Ratcheting is the phenomenon of strain accumulation during asymmetric cyclic loading of metallic materials under application of non-zero mean stress at different stress amplitudes [4]. It can deteriorate the performances of components due to cumulative effect of fatigue damage and accumulation of permanent ratcheting strain, which can lead to further enhancement of fatigue damage by continuous thinning out of the components' cross-sectional area, and their combined effect can lead to premature failure of the material [5].

About in the year 1911, Bairstow [6] introduce a new phenomenon calling it cyclic creep phenomenon and started research on it. In this research, he studied effect of positive mean stress on the nature of strain accumulation under uniaxial cyclic stressing in steel. Thereafter in the decade of 1950s, came a burst of investigations to understand axial strain accumulation due to asymmetric uniaxial cyclic loading at elevated temperature [7–9] as well as room temperature [10–12]. During 1980's a large group of researchers showed their interest to investigate the deformation takes place due to cyclic creep in various materials and such investigations are still continue on various materials such as spring steel [13], stainless steel [14-16], Sn-Pb solders [17,18],carbon steels [19,20], copper and copper alloys [21,22], polymers [23,24] and metal matrix composites [25]. During this period, cyclic creep was terned as ratcheting. A detail study of investigations related to ratcheting revels that all these research works are mainly focused on

influence of different test parameters viz. mean stress, maximum stress [14], stress ratio [26], temperature [27] etc, whereas effect of behavior of materials like cyclic hardenability and cyclic softenability [28, 29] and the pre-strain effect on ratcheting [30] was also studied by few investigators. Most of the investigations are mainly experimental analysis of the uniaxial and multiaxial ratcheting behavior of various materials subjected different loading conditions. Review of the existing literature concludes that ratcheting behavior of any material mainly depends on material types, cyclic softening and hardening behaviors of materials and loading history of such materials [14, 31].

Aluminum 7075 alloy is mainly used in aerospace structures, automobile parts where they are subjected to such loading conditions that there may be presence of fatigue loading which are of asymmetric kind in nature during service. While designing these structures on the basis of strain-controlled fatigue life estimates, may not be provided with necessary safety level. Therefore it is necessary to study the type of strain accumulation due to ratcheting in this material. Further, the material is age hardenable and hence it is also of practical importance to study the effects of aging on the ratcheting behavior of the material. The outcome of this research may enhance the level of safety of critical structures as well as enrich literature.

## 1.2 Objectives of the research work

The objectives of the proposed investigation are as follows:

(a) To characterize the selected alloy in terms of its microstructure, hardness and tensile properties.

(b) To investigate the effect of various combinations of stress parameters on the ratcheting behavior of the selected alloy.

(c) To examine post-ratcheting tensile behavior of the material.

# Chapter 2

# Literature Review

# *Literature review*

## 2.1 Introduction

Ancient Romans and Greeks used aluminium salts as dyeing mordants and as styptics for dressing wounds. *Humpry Davy* in 1808 identified the subsistence of an alum base metal and named it first *aluminum* and later on *aluminium* [32]. *H. Sainte-Claire Deville* first produced aluminium from reduction of aluminium chloride with sodium in 1855 in France. *Hall-Héroult* introduced Hall-Héroult process by dissolving the alumina in molten cryolite (Na3AlF6) in 1886. Later on in 1888, *Karl Josef Bayer* first patented the Bayer process (digesting crushed bauxite in strong sodium hydroxide solution at temperatures up to 240°C [32].

Aluminium is a soft, silver white, ductile, light weight, high electrical conductivity and non-magnetic metal. It has noteworthy low density and excellent corrosion resistance because of the phenomenon of passivation/ because of its passive nature. These properties enable it and its alloys to put into use in structural components in aerospace industries. It is used in many sectors such as transportation, packaging, construction, electrical transmission lines for power distribution, heat sinks for electronic devices such as transistors and CPUs etc. Pure aluminium is only used where workability and/or corrosion resistance is more significant than strength or hardness. The most common alloying elements are copper, magnesium, manganese, silicon and zinc [33].

## 2.2 Types of aluminium alloy

There are two types of aluminium alloy

(a) Wrought alloy (b) Cast alloy

### 2.2.1 Wrought aluminium

The International Alloy Designation System is the most extensively acknowledged naming convention for the wrought alloys. Wrought aluminium is known with a four digit number which identifies the alloying elements. Here the first digit indicates the major allying element.

| | |
|---|---|
| 1000 series | Pure Aluminium with minimum of 99% of Aluminium by weight. These can be work hardened. |
| 2000 series | Copper – major alloying element. These can be precipitation hardened to increase strength however susceptible to stress corrosion cracking |
| 3000 series | Manganese – major alloying element. These can be work hardened. |
| 4000 series | Silicon – major alloying element. |
| 5000 series | Magnesium - major alloying element. |
| 6000 series | Magnesium & Silicon - major alloying element. These are weldable, easy to machine and can be precipitation hardened to increase strength. However strength is less than 2000 and 7000 series. |
| 7000 series | Zinc - major alloying element. These can also be precipitation hardened however the highest strength of any Al alloy can be acquired. |
| 8000 series | Other elements as alloying elements which are not covered in other series. |

### 2.2.2 Cast Alloys

Cast aluminium alloys use a four to five digit number with a decimal point. The Aluminum Association (AA) has followed a classification related to that of wrought alloys. In the AA system, the second two digits correspond to the minimum percentage of aluminium. The digit after the decimal accepts a value of either 0 or 1, indicating casting and ingot respectively. The major alloying elements present in the AA system are as follows:

- 1xx.x series minimum 99% aluminium
- 2xx.x series copper
- 3xx.x series silicon, magnesium and/or copper
- 4xx.x series silicon
- 5xx.x series magnesium
- 7xx.x series zinc
- 8xx.x series tin
- 9xx.x series other elements

The wrought aluminium alloy series is again subdivided into two sections depending on physical and mechanical properties.

## 2.3 Non-heat treatable alloy

The three series 1xxx, 3xxx and 5xxx are non heat treatable alloy. The strength of these alloy increase by cold working or strain hardening example as rolling, drawing through dies, stretching or similar operation where reduce the area.

**1xxx:** 1xxx series alloy are pure with no less than 99 % aluminum [33]. They have super ordinate corrosion resistance, highly reflective and decorative, very high electrical conductivity and warm ,The mix of these properties builds these alloys extremely suitable for bundling electronic gadgets , warming equipment , lighting applications and adornment , amongst others. it has Very low strength, because there are minimum solute or encouraged combination component species present, fewer boundaries against dislocation mobility. The fundamental contamination components are Fe and Si (under 1 %).

**3xxx:** Manganese, the fundamental alloying element in 3xxx series (go 1–2 wt%), makes the combination flexible, bringing about great formability while as yet permitting an extensive variety of mechanical properties through different strain hardened tempers. The 3xxx arrangement is medium quality alloy. An extremely ordinary application is the drink can body because of the compounds great formability by squeezing, roll drawing and framing. Additionally application is bundling, building and home machines. This arrangement compounds perform well with their generally high thermal conductivity consolidated with medium quality and corrosion resistance and can hence be utilized as heating equipment as a part of brazing sheet, heating tubes etc.

**5xxx:** Magnesium as the main alloying component in the 5xxx series (utilized around 6 wt %) prompts solute hardening of alloy and effective strain hardening, bringing about medium quality. These compounds have better formability and quality when contrasted with the 3xxx arrangement composites. With the exception of the defenselessness to intergranular consumption under extremely unfavorable conditions (when Mg > 3 wt %), the 5xxx arrangement composites have great consumption execution, particularly their resistance in seawater and marine climate is

better than other amalgam arrangement. There are numerous applications as open air presentation as in building construction modeling sheet and particularly marine applications (boat building, stages, and so forth). Likewise in auto, the 5xxx arrangement compounds are utilized for press framed body-parts and undercarriage segments because of their great blend of strength and formability.

## 2.4 Heat treatable aluminium alloy

The 2xxx, 6xxx and 7xxx series are heat treatable aluminium alloy. The strong solvency of alloying component in aluminum increases with the increment in temperature thus it is possible to get extra strength in the heat-treatable alloy by subjecting them. To an elevated thermal treatment, quenching and aging at specified temperature also known as artificial aging.

**2xxx:** In this series of alloy has Cu is the main alloying element. Also some element such as Mg and Pb are present to form a strengthening precipitate so its increases the strength of alloy. These alloys have very good fatigue properties. Due to high strength, there are many applications such as aircraft fittings and wheels, forgings for trucks, military vehicles and bridges, etc. The some low melting phase elements have present such as lead and/or bismuth, which is facilitate for machining , so its uses where hard extruded machined parts are required (screws, bolts, fittings, machinery components, etc) .

**6xxx:** Si and Mg (mostly in the range 0.3–1.5 wt% Si and Mg) are the major alloying elements. 6xxx series are high strength alloys that can be strengthened by heat treatment. These alloys have low strength as compared to 2xxx and 7xxx series of alloy, but they have good weldability,

formability, excellent corrosion resistance. These alloys have excellent properties therefore its use in lots of applications as transport, building, marine, heating, brazing sheet, etc.

**7xxx:** 7xxx series are very strong alloys. The major alloying element is Zn. This is a heat treatable alloy which strength increases by precipitation hardening. The Zn (4-6 wt %) and Mg (1-3 wt %) have presented to form a strengthening precipitate but less corrosion resistance. These alloys have superior strength, so it critical application such as space exploration, aerospace, military and nuclear applications, building applications, ski poles, tennis rackets etc. However, decrease the corrosion resistance due to the additions of zinc and magnesium.

**4xxx:** Si is the main alloying element of 4xxx series alloy. These are heat treatable and non heat treatable alloy in nature. They have low ductile properties due to Si content (up to 12%) which is form a intermetallics precipitates to making the material brittle. These alloys have limited application as wrought product because of lower melting point as compare core alloy. These alloys are widely used in foundry industry because there have high fluidity properties, shrinkage defects reduce of the cast product.

**8xxx:** This series have few different elements like Li, Ni, Fe, and Si present. The combinations of these elements are separately with aluminum to make different types of alloy of this series.

Some example like Al-Li alloys used as aerospace industry, alloy with 1% Fe applied for making foil etc. These alloys have outstanding resistance of fatigue crack growth so it's used as aerospace industry. These properties of alloys have due to presence of ordered $LiAl_3$ precipitates in coherent form.

## 2.5 Temper designations

Here, the wrought or cast alloy designation is followed by a dash, a letter and a one – three digit number [33]. The designations of the tempers are:

- F As fabricated
- H Strain hardened (cold worked) with or without thermal treatment
- O Full soft (annealed)
- T Heat treated to produce stable tempers
    - T1 Cooled from hot working and naturally aged (at room temperature).
    - T2 Cooled from hot working, cold-worked and naturally aged.
    - T3 Solution heat treated and cold worked.
    - T4 Solution heat treated and naturally aged.
    - T5 Cooled from hot working and artificially aged (at higher temperature).
    - T6 Solution heat treated and artificially aged.
    - T7 Solution heat treated and stabilized.
    - T8 Solution heat treated, cold worked, and artificially aged.
    - T9 Solution heat treated, artificially aged and cold worked.
    - T10 Cooled from hot working, cold-worked, and artificially aged.

### 2.5.1 T6 process

It is a temper designation which does for improve its mechanical properties of material. The temperature and time have taken for this treatment which is depends on material. Solution heat treatment of the alloy was done at 470$^{o}$C for 1 hour, followed by rapid quenching in water and

finally artificial aging at 120$^{o}$C for 24 hours, which was followed by air cooling up to room temperature [34].

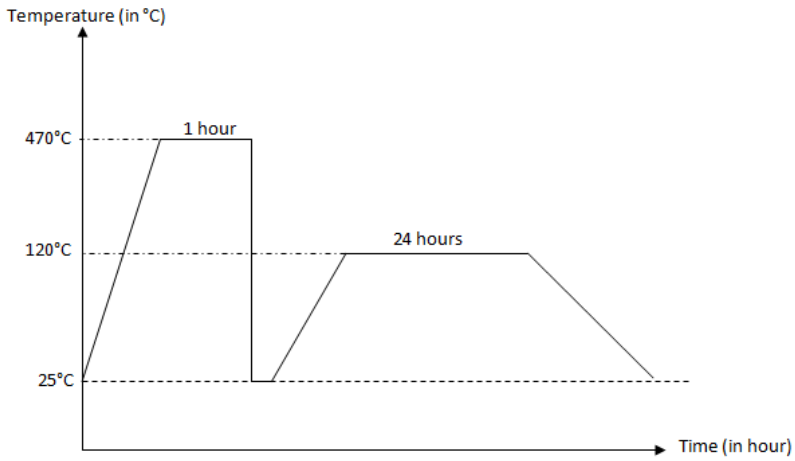


**Fig.2.1**: Schematic diagram of T6 treatment for aluminum 7075 alloy

## 2.6 Fatigue

Fatigue started to exist in the 1800s as a result of various accidents connected with railroad axles and spans, both of which were subjected to cyclic loading. Today any pivoting and moving parts of machinery application are failure by fatigue, like a compressor, wheel, turbine, axel, car chassis, pressure vessel, crane, load bearing structure, and pipe. It is very much acknowledged today that all most 90 percent of the all service failure takes place due to fatigue [3].

Cyclic loading affects due to applying loading direction changes with time. If the load is applied very less during cyclic loading then material deforms only in elastically and if applied load is low enough that the material deforms elastically and exists a high number of cycles which is called as high cycle fatigue (HCF). Then again, if employed cyclic load is sufficiently high to change the initial condition of material plastically and hold up comparatively low number of

cycles before failure is known as low cycle fatigue (LCF). Materials reaction under cyclic loading (i.e. combined HCF and LCF) is termed as fatigue. The numerous stage process for fatigue failure are beginning the initiation of cracks , propagations of initiated cracks and lastly, it prompted to failure of parts of machinery or component [35].

The fatigue promoted by:

- Interruption in crack growth
- Change in oxidation and corrosion conditions
- Change in stress amplitude
- Overload and accompanying retardation of crack

### 2.6.1 High cyclic fatigue

HCF generally called for high frequencies in excessiveness of around 1 kHz. Maybe a superior meaning of HCF would be a condition of fatigue high number of cycles quantity to failure (generally > $10^4$ cycles). A prominent definition is kept away from where purely elastic behavior is related with HCF while LCF implies cyclic plasticity. Designing meaning of HCF can be communicated as; alternating load may be such that maximum stress should not be greater than the 2/3 of yield stress of the material [Nicholas 2006]. HCF generally carried out in load or stress control mode while LCF is usually carried out in strain-controlled condition. There is no any conventional definition, but HCF generally includes high frequencies, nominally elastic cyclic behavior, low amplitudes, and endures large numbers of cycles.

### 2.6.2 Low cyclic fatigue

Low cycle fatigue is the most important consideration part of any cyclic loaded part as machinery component, pipe line, airplane etc where the applied high amplitude of stress at

minimum number of cycle. The ahead of time of fatigue work of Coffin [Coffin 1954] and Manson [Manson 1953] in the fifties. Low cycle fatigue is occurs in every cycle act as macroscopic plastic deformation. Example of structures where the low cycle fatigue (LCF) can be important part are pressure vessels which is pressurized only a less number cycles in many years, the power generator which is operated at elevated temperature and finding significant thermal stress, nuclear power plant where used pipe lines. The numbers of considerable pressurized/depressurized (on/off) cycles, earth quake can be LCF should be studied. Low cycle fatigue can be divided as both strain controlled and stress controlled, but strain controlled process is more usual.

The plot of lcf result as Δεp against N .The graph is plotted as log-log coordinates which is shown in Fig. 2.2 according to Coffin-Manson relation:

$$\frac{\Delta\varepsilon_p}{2} = \varepsilon_f^{'}(2N)^{C_1} \qquad (1)$$

Where:

$\Delta\varepsilon_p /2$ = plastic strain amplitude;

$\varepsilon_f'$= empirical constant as fatigue ductility coefficient, in single reversal

2N = number of reversals cycles to failure (N cycles);

$C_1$ = empirical constant as fatigue ductility exponent, generally ranging from -0.5 to -0.7 for metals.

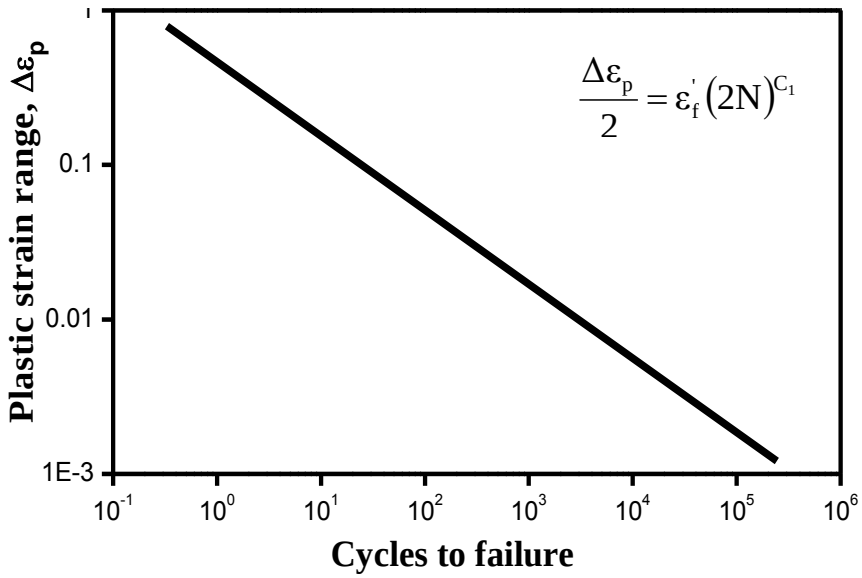


**Fig. 2.2 :** LCF graph, ($\Delta\varepsilon_p$ vs. N).

## 2.7 Mean stress and its effect on fatigue

There are huge quantities of fatigue information in literature for states of completely reversed cycle (zero mean stress). There are a few systems for deciding a S-N graph for a circumstance where the mean stress is not equivalent to zero. The Fig.2.3 demonstrates the plans that are utilized to make note of mean stress in depicting the endurance limit. Figure.2.3 is known as the Haig-Soderberg curve.

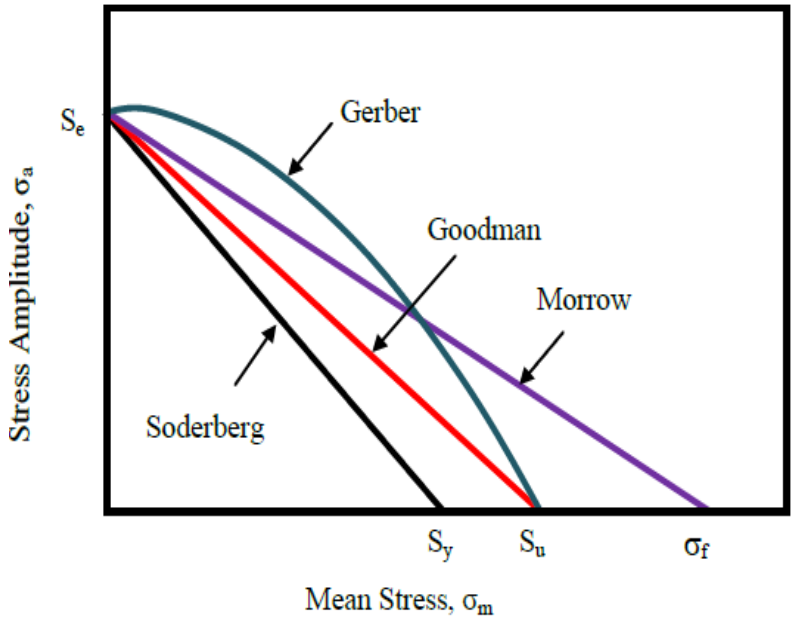


**Fig. 2.3:** Mean stress variation with respect to stress a amplitude at fatigue endurance

## 2.8 Low cycle fatigue under stress control mode: Ratcheting

Ratcheting is one type of low cycle fatigue (LCF) under stress control, where accumulation of plastic strain takes place during asymmetric cyclic loading of metallic materials. It may be considered as one of the serious issues in critical engineering sectors because accumulation of ratcheting strain decreases fatigue life of structures and components. The schematic representation of the ratcheting procedure is represented in Fig.2.4.

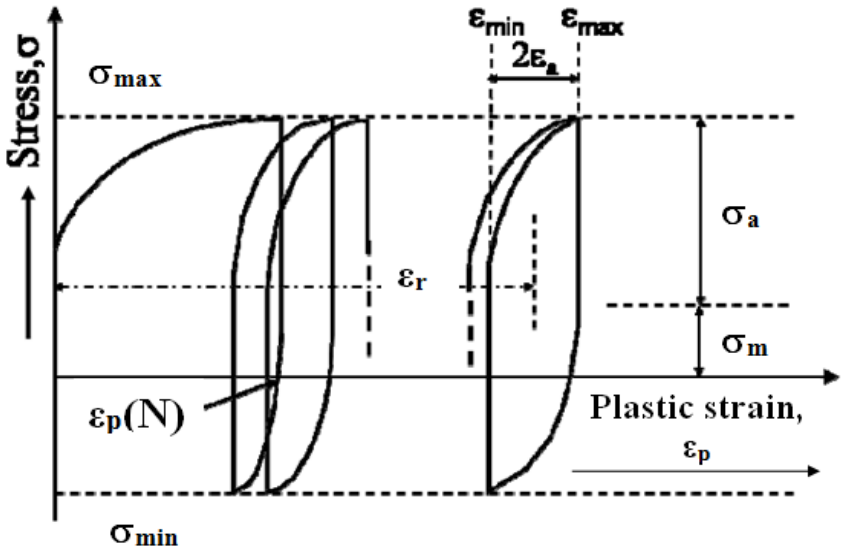


**Fig.2.4:** Asymmetrical cyclic loading at positive mean stress

Where,

$\sigma_{max}$ = Maximum stress, $\sigma_{min}$ = Minimum stress, $\sigma_m$ = Mean stress, $\sigma_a$ = Stress amplitude.

Ringsberg [36] stated that ratcheting is instances where the exhibits additional plastic deformation during every load cycles and strain accumulates continuously the material fails. Ratcheting strain can be measured numerically as mean strain at a particular cycle and can be expressed as follows [16, 17, 28, and 37]:

$$\varepsilon_r = (\varepsilon_{\max} + \varepsilon_{\min})/2 \quad (2)$$

Where $\varepsilon_r$ is axial ratcheting strain, $\varepsilon_{max}$ is maximum strain at particular cycle and $\varepsilon_{min}$ is minimum strain at that cycle.

### 2.8.1 Ratcheting history

Study on ratcheting behavior of material may be begun after the work of Bairstow [5], who reported that the accumulation of stain in steel takes place when subjected to uniaxial cyclic loading with a positive mean stress. Around then a new term called “cyclic strain accumulation" is used to describe this phenomenon. In the decade of 1950s, a lot of investigation came reporting the strain accumulation due to uniaxial asymmetric cyclic loading at elevated temperature [38, 39, 8, and 9] as well as at room temperature [10-12]. Accentuation was given to interpret the phenomenon under multi-axial non relative cyclic loading as reported by Jiang and Sehitoglu [19].

After 1970s, researchers show their interest towards the investigations to identify the effect of various parameters and also material characteristics on ratcheting phenomenon. Lorenzo and Laird [21] reported correlation between the nature of the strain accumulations in poly-crystalline copper with static creep and grouped this phenomenon in two parts as "cyclic creep acceleration" and "cyclic creep retardation". In 1990, Yoshida [26] reported the impact of stress ratio on uni-axial and multi-axial ratcheting strain accumulation in SUS304 stainless steel at room temperature. In the same year Ruggles and Krempl [40] show the interaction between cycling hardening and ratcheting for AISI 304 stainless steel. Hassan and Kyriakides [28] examined ratcheting behavior of consistently hardenable and softenable materials under uniaxial cyclic loading and concluded that material qualities incorporate cyclic hardening/softening. Later in

1996, the effect of mean stress and ratcheting on the fatigue life of steel was described by Xia et al. [41].

After 2000 onwards numerous investigations have been done on various materials viz. metals, compounds, polymers, etc. to understand their ratcheting behavior. Van and Mounmi [42] evaluate the damage takes place on pressurized pipelines due to ratcheting and fatigue under seismic loading condition. Kang et al. [27] in 2002 reported uniaxial cyclic ratcheting and properties of plastic flow of SS304 at the room as well as elevated temperature. Development of dislocation pattern and internal stresses during the cyclic creep process was reported by Gaudin and Feaugas [37]. Tao and Xia [43] examined the variation in the fatigue life of epoxy polymer under ratcheting. Deformation under ratcheting of super-elastic and shape memory Ni-Ti alloy has been investigated by Kang et al. [44]. Recently, Dutta et al. [46] in 2010 and Dutta and Ray [45] in 2013, reported the influence of ratcheting strain on 304LN stainless steel and interstitial free steel (IF) respectively.

## 2.9 Variations in ratcheting strain

Strain accumulation under ratcheting is influenced by various parameters. The main effecting parameter is types of loading which specified as man stress, stress amplitude, maximum stress, rate of stress, stress ratio, cyclic hardening and cyclic softening behavior.

### 2.9.1 Effect of stress parameter: mean stress and stress amplitude

Various groups of investigators [21, 27-29, 47] have reported on the presence of positive or negative mean stress which effects the strain accumulation under ratcheting. Variation of ratcheting strain with number of cycles at different mean stress levels is reported by many

researchers. They reported that there is a decrease in ratcheting strain takes place with an increase in mean stress. Lim at al. [22] examined the nature of strain accumulated during ratcheting under positive to negative mean stress on copper alloy. It also concludes from various investigations that applied mean stress and their sign play an important role in the increase or decrease of ratcheting strain. Also, both strain accumulation and life of material under ratcheting increases with tensile mean stress at constant stress amplitude. Strain accumulation paths are opposite to each other in case of tensile and compressive mean stress.

### 2.9.2 Effect of stress ratio

Stress ratio, which is the ratio of minimum to maximum stress ($R = \sigma_{min}/\sigma_{max}$) is one of the parameters influencing ratcheting deformation under asymmetric loading of a material. Few researchers [20,26] studied the effect stress ratio on the nature of the strain accumulation due to ratcheting. Yosida [26] reported that when the value of R is negative or positive or zero, there is a significant amount of ratcheting strain is accumulated in the material. But whem R= -1, i.e. at zero mean stress, no chance of the accumulation of ratcheting strain. One can clearly understand the variation in ratcheting strain at different R value from the Fig.2.5.

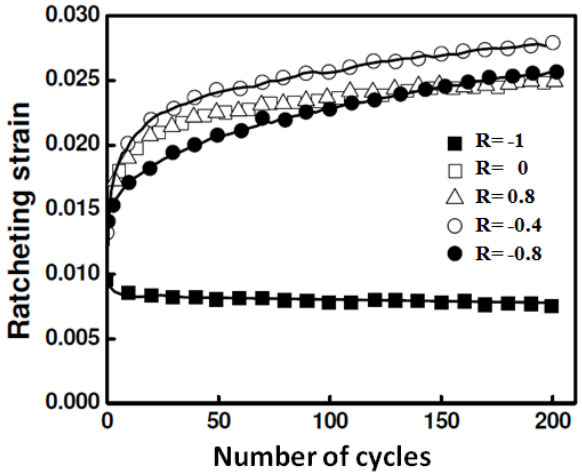


**Fig.2.5:** stress ratio effect on accumulation of ratcheting strain

### 2.9.3 Effect of cyclic hardening /softening

The behavior of cyclic hardening and softening are depend on initial stage of material and applied cyclic loading like stress amplitude, mean stress and temperature [48].Generally, soft material shows cyclically harden and hard material show cyclically soften [49]. Ratcheting conduct of the material relies on upon cyclic hardening / softening highlights of the material. Kang et al. reported of 25CDV4.11 which is shows cyclic softening behavior and SS304 stainless steel which is show cyclic hardening behavior [29].They also reported that softening behavior material during cyclic loading increases the ratcheting strain with number of cycles and hardening behavior of material during cyclic loading decreases the ratcheting strain with increases the number of cycle.

## 2.10 Re-appraisal of the current problem

In recent years, one of the most important alloys used in aerospace industry, automobile industry etc. is aluminium 7075-T6 alloy because of its suitable properties. From application point of view of the alloy, it is crucial to understand the fatigue behavior of the material such that maximum safety can be imparted to the components used in critical sectors. After a detailed literature survey it was found that no reports exist, which deal with the ratcheting fatigue behavior of the alloy. Hence, the current investigation is intended to study the ratcheting behavior of aluminium 7075-T6 alloy to fulfill this gap.

# Chapter 3

# Experimental Procedure

# *3. Experimental procedures*

## 3.1 Introduction

The aim of this investigation is to study the cyclic deformation behavior of an aluminium 7075-T6 alloy. To carry out of these objectives, different kinds of experiments were conducted which are described in this chapter. An overview of all the experiments includes determination of chemical composition of the selected steel, heat treatment, microstructural characterization, determination of the tensile behavior of the alloy, study of fracture surfaces, experiments related to stress-controlled asymmetric cyclic fatigue (ratcheting) behavior, ratcheting followed by tensile tests and X-ray diffraction studies on ratcheted samples.

## 3.2 Material selection and chemical composition

Aluminium 7075-T6 alloy was selected for this investigation. The aluminium 7075 alloy was received in the form of rods of 16 mm diameter. The chemical composition of the material was assessed using optical emission spectrometer (Model: ARL 3460 Metals Analyzer).

## 3.3 Heat treatment

The 7000 series Aluminium alloys are heat treatable alloys whose mechanical properties such as hardness, corrosion resistance and strength may increase and hence can be used for various purposes according to their requirement. LI Jin–feng has studied the effect of the various heat treatments on 7000 series alloys. He reported that the strength of the alloy increases if solution heat treatment with aging (T6) is imparted [50]. Following LI Jin-feng , solution heat treatment of the alloy was done at 470$^{o}$C for 1 hour, followed by rapid quenching in water and finally

artificial aging at 120$^{o}$C for 24 hours, which was followed by air cooling up to room temperature [34].

**Fig**. 3.1: Image of specimens during heat treatment

## 3.4 Microscopic examinations and image analyses

Cylindrical samples of 16 mm diameter with 10 mm (approx.) height were cut from the heat treated material for metallographic examinations. All samples were initially polished with different grades of emery papers (1/0, 2/0, /3/0 and 4/0), cloth polisher with alundum solution and finally using 0.25 μm diamond paste. To get a better view of the grain boundaries, electro polishing has also been done to the work-piece. In electro polishing method, a stainless steel rod was chosen as cathode whereas the sample was kept as anode with phosphoric acid as

electrolyte. Firstly the phosphoric acid was heated up to 70$^{o}$C for its use as an electrolyte, following [51]. The current density and voltage were kept as 100 mA/cm$^2$ and 12 V respectively. The electro polishing of the sample was done for 10 minutes. The samples were washed with distilled water after the electro polishing. The polished specimens were etched by the freshly prepared Keller's reagent [2 ml HF (1%), 3ml HCl (1.5%), 5 ml $HNO_3$ (2.5%) and 190 ml $H_2O$ (95%)].

The microstructures of the investigated materials were examined using an optical microscope (Model: ZEISS Axiocam ERc 5s) connected to an image analyzer and a series of representative photographs were recorded. The average grain size was estimated using a linear intercept method following ASTM standard E-112 [52]. In this method, a linear test pattern was laid over on the optical microstructure, and calculates the grain intercepted by test line was numbered. Such measurements were repeated at least on ten randomly chosen fields. The grain size ($d$) was determined as:

$$d = \frac{L_T}{N_L}$$

Where, $N_L$ = No. of intercepted grains by a unit line true test length. The true length $L_T$ of a test line is considered as the line length of the test at unit enlargement.

## 3.5 Hardness

The cylindrical samples of 16 mm diameter with an approximate height of 10 mm were cut from the as received and heat treated materials for determination of Vickers hardness. The hardness measurements of aluminium alloy were made at indentation load of 5 kgf and 10 kgf. These tests

were carried out using a Vickers hardness testing machine (Leco, Model: LV 700, Michigan, USA) for a dwell time of 10 s. Ten readings were taken to estimate their average hardness values.

## 3.6 Tensile test

Tensile tests were carried out using cylindrical specimens having 6 mm diameter and 25 mm gauge length following ASTM standard E8M-08 [53]. The specimens were fabricated from the obtained rods of aluminum 7075-T6 alloys. A typical configuration of a tensile specimen is shown in Fig.2. All tests were carried out using cross-head velocity of 1 mm/min with the help of a universal testing machine (Instron 1195, Birmingham, UK) at room temperature.

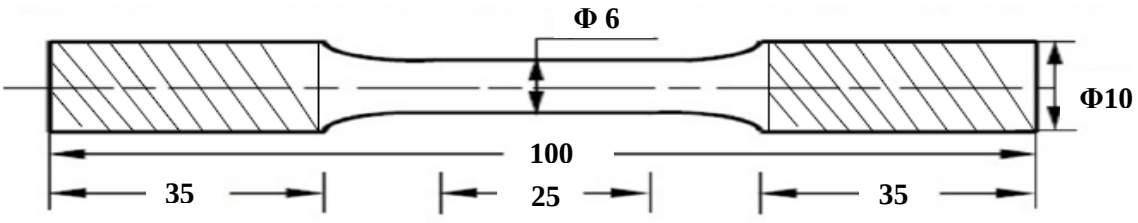


**Fig.3.2**: Sample design for tensile test

At least three tensile tests were carried out on fabricated tensile samples to estimate the average tensile properties. The stress-strain data were recorded during the tests for subsequent analyses.

## 3.7 Ratcheting test

The ratcheting tests were carried out using cylindrical specimens having gauge length 13 mm and diameter 7 mm as per ASTM standard E606 [54]. The specimens were fabricated from the heat treated rods and no heat treatment was done after fabrication of samples. A schematic drawing of a specimen for ratcheting test is illustrated in Fig.3.

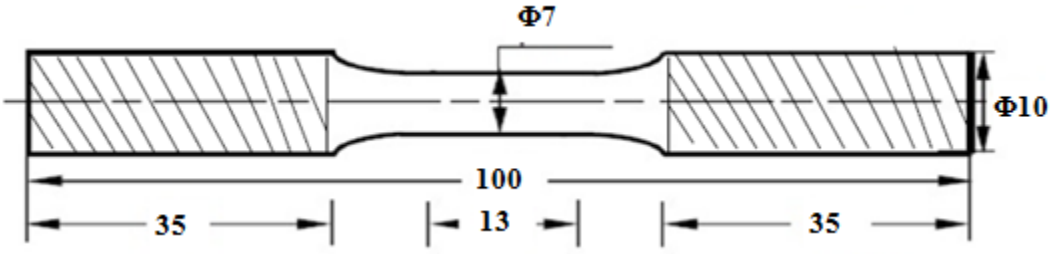


**Fig.3:** Sample design for fatigue test

Stress controlled ratcheting tests were carried out at room temperature up to 100 cycles using ±250 kN servo-hydraulic testing machine (Model: INSTRON 8800R). All the tests were done at a constant stress rate of 5 MPa/s. The variables that have been considered for these tests are mean stress ($\sigma_m$) and stress amplitude ($\sigma_a$). Test matrix parameter for the alloy is given in Table 1. The test control can be classified into two categories (i) constant mean stress($\sigma_m$) with varying stress amplitude($\sigma_a$) (ii) constant stress amplitude($\sigma_a$) with varying mean stress ($\sigma_m$). Further, it can be stated that the chosen test parameters were such that all the tests fall in tension-tension zone. During each test the actuator displacement as well as the load-extension data was uninterruptedly recorded by using attached software to the computer. It was aimed to produce at least 200 data points per cycle during tests.

**Table 1:** Test matrix for fatigue test of fabricated sample

| Serial no. | Mean stress ($\sigma_m$), MPa | Stress amplitude ($\sigma_a$), MPa |
|---|---|---|
| 1 | 55 | 25 |
| | | 35 |
| | | 45 |
| 2 | 65 | 25 |
| | | 35 |
| | | 45 |
| 3 | 75 | 25 |
| | | 35 |
| | | 45 |

## 3.8 Post ratcheting tensile tests and fractographs

The post ratcheting tensile tests were carried out on ratcheted specimen as discussed in section 3.6.where the cross head velocity where 1mm/min. The fractured surfaces were cut out carefully from the broken tensile specimens. Fractography studies were carried out by using scanning electron microscope (Model: JEOL-JSM 6480LV). The elemental analysis of inclusion on the fracture surface was carried out by energy dispersive spectroscopy (EDS), attached with the FESEM.

## 3.9 X-ray diffraction

To determine whether the investigated materials contain any distinguishable second phase, X-ray diffraction examinations were carried out. Representative samples were analyzed using CuKα radiation of a high-resolution X-ray diffractometer (Model RIGAKU JAPAN/ULTIMA-IV). The specimens were scanned to generate X-ray diffraction patterns in the 2θ range 30 – 100°, with a step size of 0.05° and scan rate of 10°/min.

# Chapter 4

# Results and Discussion

# *Introduction*

4.1 Introduction

Ratcheting behavior of aluminum 7075 –T6 alloy was investigated in this study up to a specified number of cycles; this was followed by studying the post ratcheting tensile behavior of the alloy. To full fill the objective of these investigation first ratcheting test were carried out under stress controlled asymmetrical cyclic loading by varying mean stress and stress amplitude during the test for 100 cycles of loading. The necessary details of all the test procedures are given in chapter 3. On completion of ratcheting tests, tensile tests were carried out on the all previous ratcheted specimens.

In this chapter, the obtained results of the all tests are incorporated along with their pertinent analyses. The results pertaining to basic material characteristics are also discussed in the first few sections of this chapter.

## 4.2 Chemical composition

The Aluminium 7075 alloy was received in the form of rods of 16 mm diameter. The chemical composition of the material was assessed using optical emission spectrometer (model: ARL 3460 Metals Analyzer), which is shown in Table 4.1.

Table 4.1: Chemical composition of Aluminium 7075 alloy (in weight %).

| Elements | Zn | Mg | Cu | Fe | Cr | Si | Mn | Ti | Al |
|---|---|---|---|---|---|---|---|---|---|
| Weight % | 5.203 | 2.163 | 1.856 | 0.261 | 0.256 | 0.206 | 0.087 | 0.044 | Bal. |

The presence of Zn and Mg up to about 5% and 2% respectively include the alloy in the 7000 series as per ASTM [55]. Addition of these elements in the alloy increases its mechanical

properties so that the alloy can be used in aerospace and automobile industries [33]. The other major elements, which are present in the alloy, are Cu and Cr. It is known that the material is precipitation hardenable on artificial aging and hence, presence of Cu of 1-2 % is most essential for the formation of Al and Cu based precipitates (like AlCu, $AlCu_2$ and $Al_2Cu$ etc.)[3]. Formation of these precipitates increases the mechanical properties of the alloy. This precipitates generate during aging process, which are known as Guinier-Preston zone (GP-zone) [50]. The presence of Zn and Mg in this alloy also imparts strengthening by precipitating at the grain boundaries [56].

## 4.3 Microstructural analysis

The aluminum alloy was investigated for its microstructural characterization using an optical microscope (Model: ZEISS Axiocam ERc 5s), which is connected through an image analyzer. A typical optical micrograph of the alloy is shown in Fig. 4.1. It is evident from the micrograph that elongated pancake shaped grains with uniform size are present throughout the specimen [57]. The average grain size was estimated at 11.76 ± 1.11 μm using linear intercept method following ASTM standard E-112 [52].

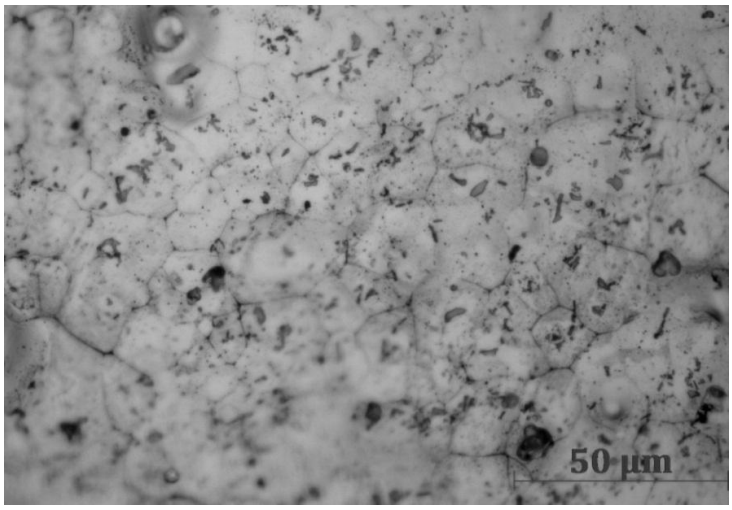


**Fig. 4.1:** Optical microstructure of 7075-T6 alloy.

## 4.4 Conventional mechanical properties

The mechanical properties of investigated Aluminium 7075-T6 alloy includes tensile properties and hardness values. Tensile tests were done using universal testing machine (Model: INSTRON, 1195) whereas, microhardness tests of the specimen were carried out using Vickers micro hardness tester.

### 4.4.1 Hardness determination

The hardness test was carried out on 2 different cylindrical specimens of 16 mm diameter with approximate length of 10 mm, which were cut from the as received and heat treated aluminum alloy respectively. The hardness measurements of selected Aluminium 7075 alloy were applied an indentation load of 5 kgf and 10 kgf. These tests were carried out using a Vickers hardness-testing machine (Leco, model: LV 700, Michigan, USA) for dwell time of 10 s. The obtained results are for 5kg load applied the hardness values of received and heat-treated alloy are 92 and 150 respectively. Similarly if 10 kg load applied the obtained value are 95 and 151±1.63 respectively.

The hardness values for as received alloy was observed to be lower than that of the T6 alloy at both loads. In T6 condition, a continuous uniform grain structure was observed (Fig. 4.1). Kumar et al. concluded that there exists Al and Cu particle rich continuous fine grain structure in the alloy. In association, precipitates like $MgZn_2$ at the grain boundaries helps to increase the hardness value. The temperatures, time and cooling rate are important factors of aging treatment, which changes the properties of the alloy. Kumar et al. studied effect of post weld heat treatment on the hardness of AA7075. They reported that hardness value of the alloy was 170 VHN for T6 heat treated condition. The composition of the current alloy is similar with Kumar et al. while the hardness values also close to their results [57].

### 4.4.2 Tensile properties

The tensile tests were carried out on samples fabricated following ASTM standard E8M [53]. The procedure of tensile test is mentioned in Section 3.6. The tensile data were obtained by using the INSTRON 1195 machine. The obtained tensile properties of the material are summarized in Table 4.2. These data were analyzed to calculate the value of yield strength, ultimate tensile strength (UTS), percentage uniform elongation ($\%\varepsilon_u$) and percentage total elongation ($\%\varepsilon_t$) of alloy. Typical engineering stress-strain curve is plotted which is shown in Fig.4.2(a) There are materials which show continuous yielding behavior from elastic to plastic region and hence it is difficult to locate their yield strength value. To avoid such difficulty, the yield strength of such material is taken as 0.2% strain offset, as per ASTM standard E8M [53].

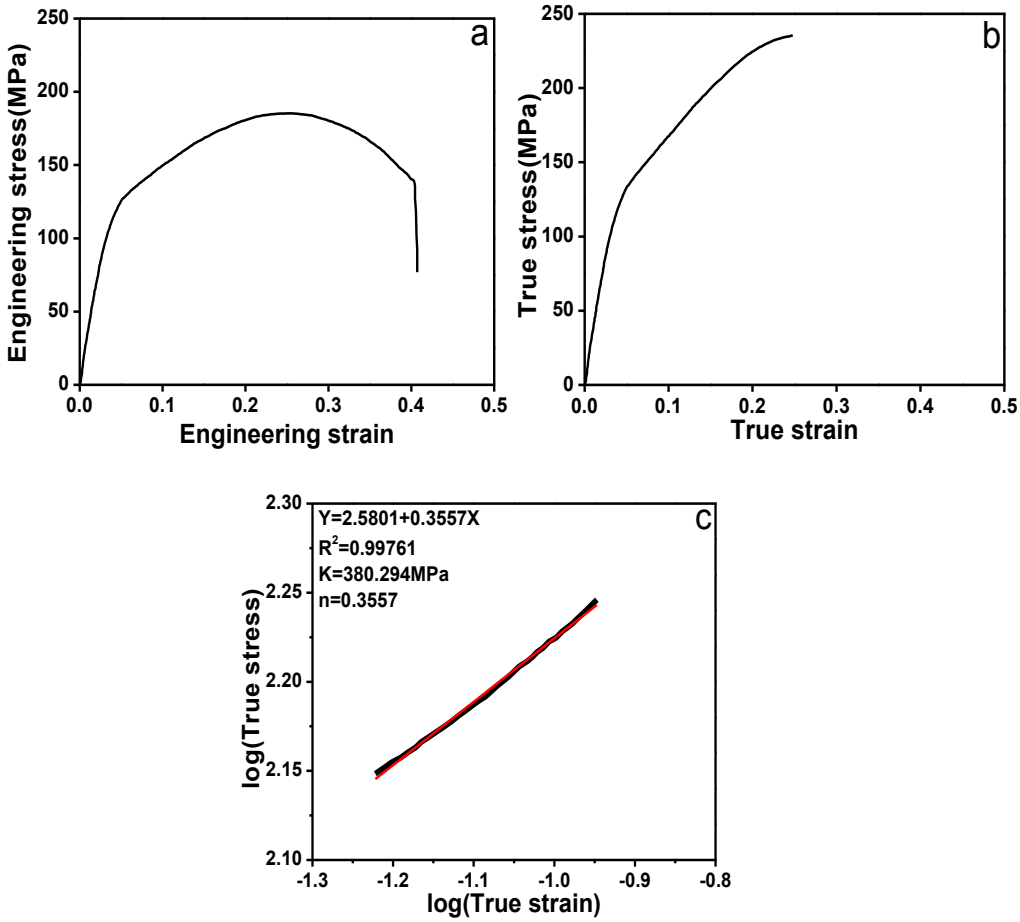


**Fig 4.2:** Typical graph of engineering stress-strain, true stress-strain and log-log plot as (a),(b) and (c) respectively.

**Table 4.2:** Tensile properties of Aluminum 7075-T6 Alloy

| Material | Tensile strength(MPa) | Yield strength(MPa) | $\%\varepsilon_u$ | $\%\varepsilon_l$ | *n* | K (MPa) |
|---|---|---|---|---|---|---|
| Al 7075-T6 | 188 | 70 | 25.586 | 40.297 | 0.3557 | 380 |

The data obtained from the engineering stress–strain diagram 4.2(a) was used to estimate the value of true stress(σ), true strain(ε) of the alloy and using values of σ and ε,true stress-strain curve is plotted which is shown in Fig.4.2(b) and also log (σ) vs. log (ε) was plotted, which is

shown in Fig.4.2(c). The parameters like strain hardening exponent and strength coefficient were calculated from Fig.4.2(c) using Hollomon equation $\sigma=K\varepsilon^n$, where $K$ is strength coefficient and $n$ is strain hardening exponent [3]. The values of $n$ was predicted from the slope of log-log plot and values of strength coefficient were calculated from the intercept of the plot to the y-axis (stress axis) at $\varepsilon = 1$. For the investigated alloy, the strain hardening exponent value was found to be 0.35 in the of strain range of 10-20%.

### 4.4.3 Fractography of broken tensile samples

The fracture surfaces of broken tensile specimens were examined using field emission scanning electron microscope (FESEM, Model: Nova NanoSEM/ FEI). Typical fractographs obtained from the FESEM are shown in Fig.4.3.

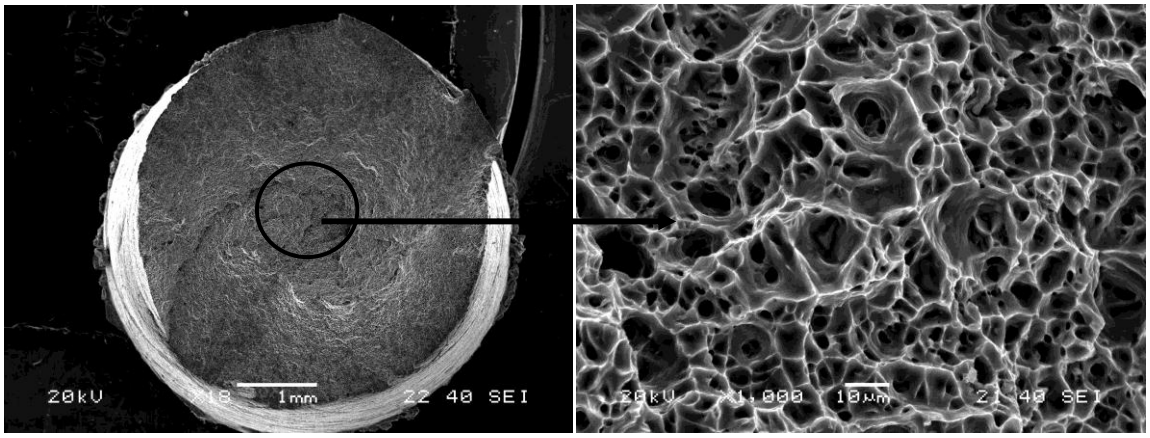


**Fig 4.3:** SEM image of tensile broken fracture surface

The fractographs reveals dimples on the surface, the typical nature of fracture surface of a ductile material, as expected. The dimple fracture in aluminium alloy was observed due to presence of second phase particles in it and there is de-cohesion of the particle – matrix interphase. The

fracture surface also indicates presence of some inclusion-like particles. These were examined by energy dispersive X-ray spectroscopy (EDS) for identification of its chemical nature.

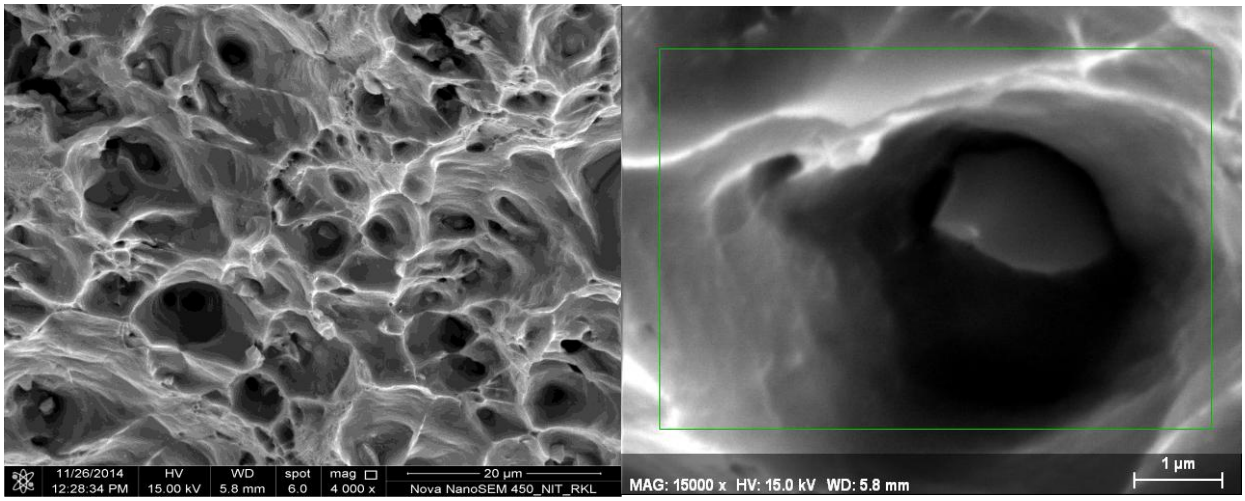


**Fig. 4.4:** FESEM image at high magnification

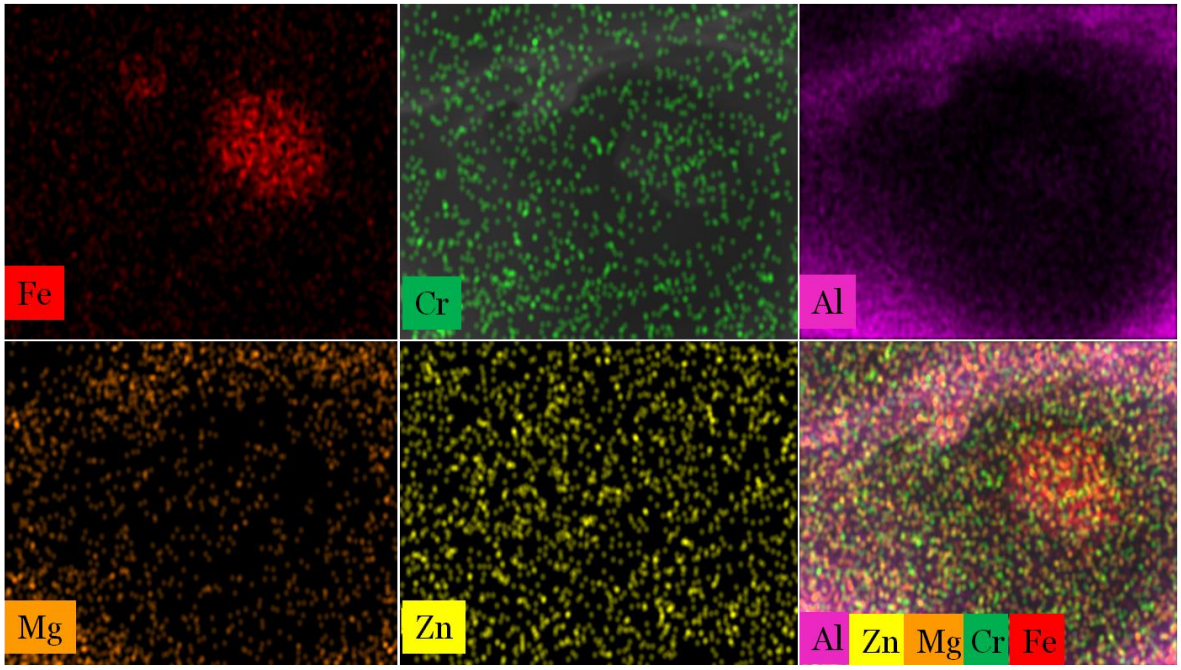


**Fig. 4.5:** Image mapping for inclusion in the material

As can be seen from the X-ray mapping images ( Fig.4.5) and the EDS spectra (Fig.4.6) that the inclusion is mainly iron based, otherwise, the entire material mainly contains Al, Mg, Zn etc. as major elements.

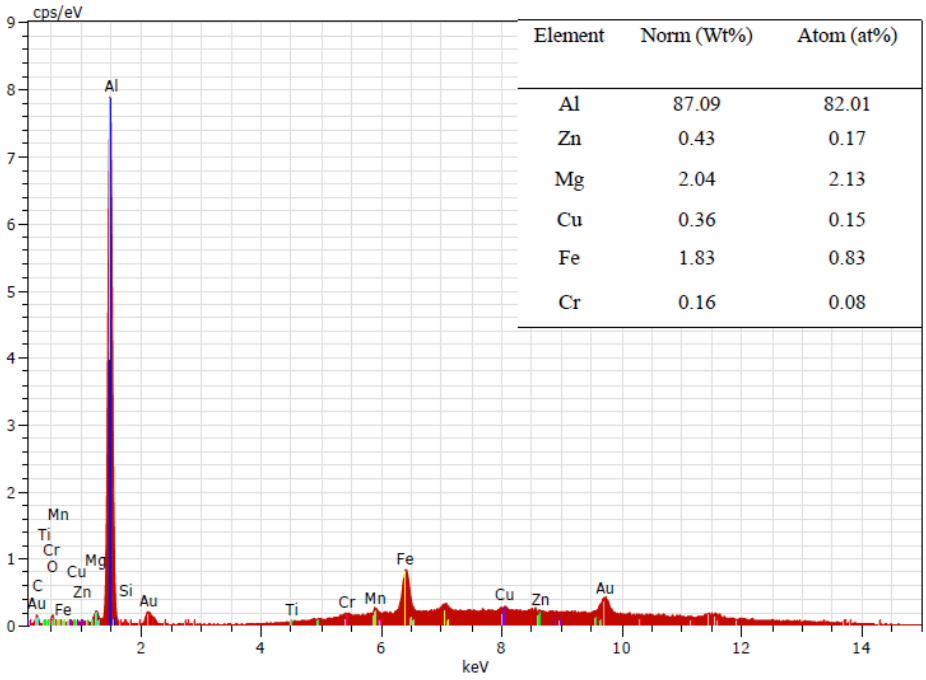


| Element | Norm (Wt%) | Atom (at%) |
|---|---|---|
| Al | 87.09 | 82.01 |
| Zn | 0.43 | 0.17 |
| Mg | 2.04 | 2.13 |
| Cu | 0.36 | 0.15 |
| Fe | 1.83 | 0.83 |
| Cr | 0.16 | 0.08 |

**Fig.4.6:** EDS spectra of inclusion present on the fracture surface

## 4.5 Uniaxial ratcheting behaviour

In this section, the uniaxial ratcheting behaviour of the investigated alloy is discussed. The tests were carried out under different combinations of mean stress ($\sigma_m$) and stress amplitude ($\sigma_a$) in such a manner that the loading happens to be of tension-tension in nature. Earlier investigations on ratcheting suggest that strain accumulation due to ratcheting attains a saturation value in the range of 50 to 100 cycles, after which the rate of accumulation of strain varies negligibly even up to failure of the material [58]. Keeping this feature into mind, all ratcheting tests in the current investigation were done up to 100 cycles, to understand the trend of strain accumulation in the investigated alloy under tension-tension mode. Particularly, in aluminum and an aluminum-based

alloy, Ravi et al. [58], Dutta, and Ray [4], respectively, reported that saturation occurs within 50 cycles.

### 4.5.1 Uniaxial ratcheting behaviour at constant mean stress with varying stress amplitudes

Results of ratcheting tests for constant mean stress and varying stress amplitudes were analysed. The ratcheting strain accumulated in the alloy under asymmetric cyclic loading at constant mean stress of 55 MPa with varying stress amplitudes 25, 35 and 45 MPa are shown in Fig.4.7 (a). Similarly plot for mean stresses of 65 MPa and 75 MPa with varying stress amplitudes are shown

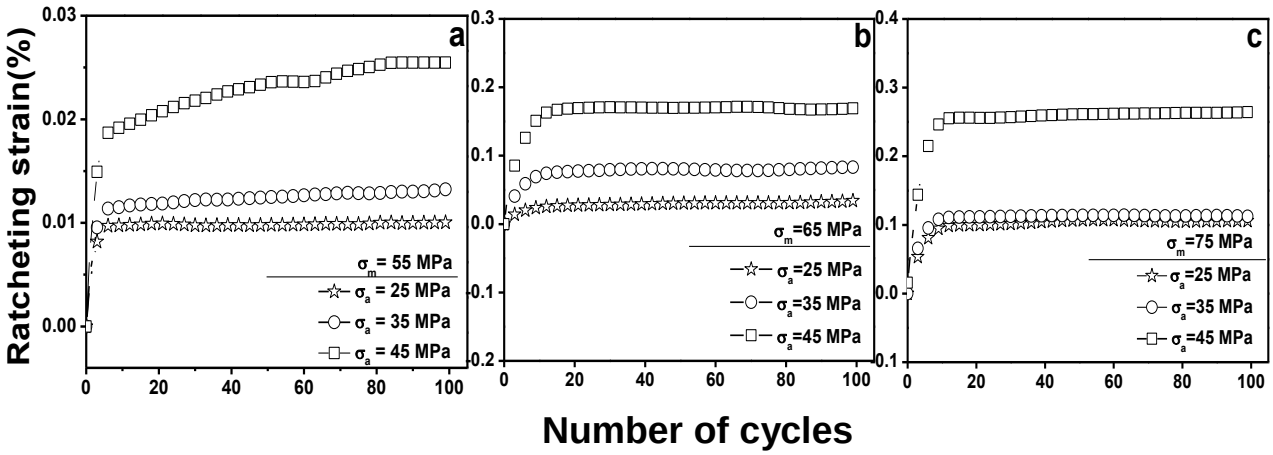


**Fig.4.7:** Typical ratcheting strain $v_s$ no. of cycle of the investigated aluminum 7075-T6 alloy: (a) at constant $\sigma_m$ = 55 MPa with varying $\sigma_a$ = 25 MPa, 35 MPa and 45 MPa.(b) at constant $\sigma_m$= 65 MPa with varying $\sigma_a$ = 25 MPa, 35 MPa and 45 MPa.(c) at constant $\sigma_m$ = 75 MPa with varying $\sigma_a$ = 25 MPa, 35 MPa and 45 MPa.

in Fig.4.7 (b) and 4.7(c) respectively.

It is observed that from Fig.4.7 that at constant mean stress with increasing stress amplitude, accumulation of ratcheting strain increases . The percentage of ratcheting strain with number of cycles at constant mean stress ($\sigma_m$) and varying stress amplitude is shown in Table 4.3.

**Table 4.3:** Accumulation of ratcheting strain at constant mean stress and varying stress amplitude

| Serial no. | Mean stress ($\sigma_m$), MPa | Stress amplitude ($\sigma_a$), MPa | Ratcheting strain,% |
|---|---|---|---|
| 1 | 55 | 25 | 0.0100 |
| | | 35 | 0.0133 |
| | | 45 | 0.0254 |
| 2 | 65 | 25 | 0.0345 |
| | | 35 | 0.0830 |
| | | 45 | 0.1695 |
| 3 | 75 | 25 | 0.1060 |
| | | 35 | 0.1120 |
| | | 45 | 0.26438 |

It is also observed from these figures that the saturation of strain accumulation takes place in the alloy after around 20 cycles under all test conditions. Initially the accumulation of ratcheting strain is sharp up to 10 cycles, which slowed down after that and finally attainment of steady state takes place after 20 cycles, for all combinations of mean stresses and stress amplitudes. Dutta and Ray investigated the nature of strain accumulation in 6063-aluminum alloy. They reported that the strain accumulation due to ratcheting depends on the remnant dislocation density [3]. The dislocation density ($4.9 \times 10^{17}/m^2$ for a loading condition of σm=40MPa,σa=165 MPa and $6.63 \times 10^{17}/m^2$ for a loading condition of σm=50MPa,σa=165 MPa) [58] increases with increasing stress parameters, i.e. with increasing ratcheting strain. The increase in ratcheting

strain for the current set of tests are can also be attributed to the increase in dislocation density, however detailed TEM study is needed for this proposition, which is not done in this investigation.

The increase in strain accumulation with increasing stress amplitude can be mechanistically expressed with the variations in the heights of the hysteresis loops and thereby corresponding deformation zone.

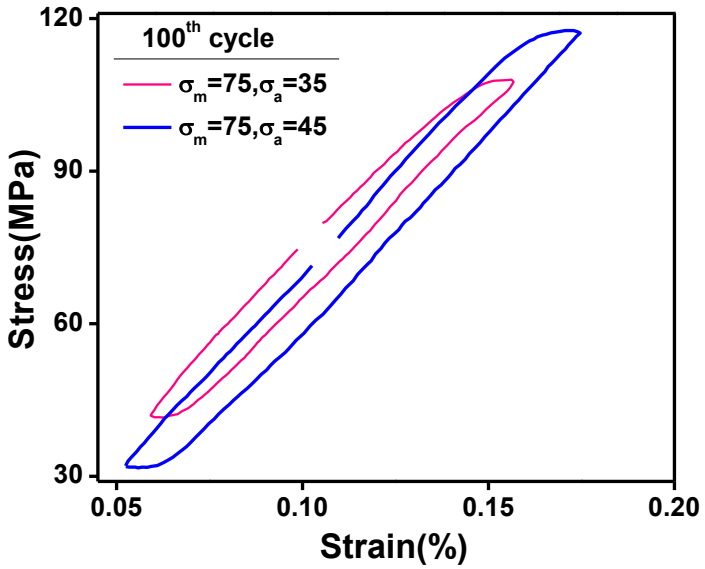


**Fig.4.8:** A typical hysteresis loop of 100 cycles loading at constant mean stress 75 MPa and varying stress amplitude 35 and 45 MPa

One can note from Fig.4.8 that the height of hysteresis loop increases with increasing stress amplitude. This fact causes more strain in a particular cycle during the cyclic loading event. On reverse loading, a part of the gathered strain is recovered while a part of strain retains in the sample as to add in the measure of ratcheting strain. Considering the phenomenon of dislocation generation, more amount of dislocations generate due to increased maximum stress during loading with higher stress amplitude.

### 4.5.2 Uniaxial ratcheting behaviour at constant stress amplitude with varying mean stress

Results of ratcheting tests for constant stress amplitude and varying mean stress were analysed. The accumulation of strain in the alloy under asymmetric cyclic loading at constant stress amplitude of 25 MPa and varying mean stress of 55, 65, 75 MPa are shown in Fig4.9 (a). Similarly, plot for constant stress amplitudes of 35 and 45 MPa with varying mean stresses are shown in Fig.4.9 (b) and 4.9(c) respectively.

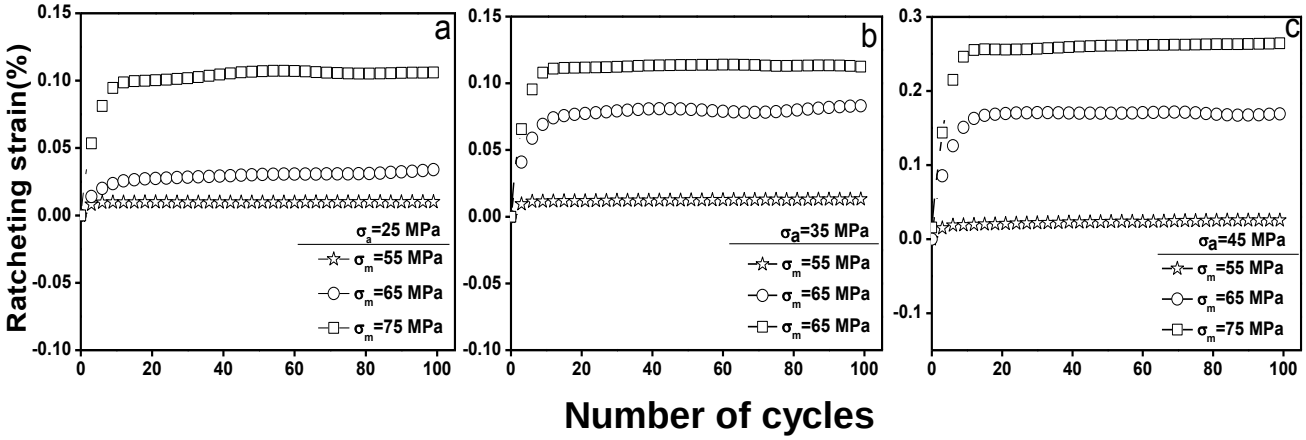


**Fig.4.9:** Typical ratcheting strain $v_s$ no. of cycle of the investigated aluminum 7075-T6 alloy: (a) at constant $\sigma_a$ = 25 MPa with varying $\sigma_m$ = 55 MPa, 65 MPa and 75 MPa,(b) at constant $\sigma_a$= 35 MPa with varying $\sigma_m$ = 55 MPa, 65 MPa and 75 MPa,(c) at constant $\sigma_a$ = 35 MPa with varying $\sigma_m$ = 55 MPa, 65 MPa and 75 MPa

It is observes that from Fig.4.9 that at constant stress amplitude with increasing mean stress, accumulation of ratcheting strain increases significantly as comparison to constant mean stress with varying stress amplitude. The percentage of accumulated ratcheting strain with number of cycles at constant stress amplitude and varying mean stress is shown in Table 4.4.

**Table 4.4:** Accumulation of ratcheting strain at constant stress amplitude and varying mean stress

| Serial no. | Stress amplitude ($\sigma_a$), MPa | Mean stress ($\sigma_m$), MPa | Ratcheting strain,% |
|---|---|---|---|
| 1 | 25 | 55 | 0.0100 |
| | | 65 | 0.0345 |
| | | 75 | 0.1060 |
| 2 | 35 | 55 | 0.0133 |
| | | 65 | 0.0830 |
| | | 75 | 0.1120 |
| 3 | 45 | 55 | 0.0254 |
| | | 65 | 0.1695 |
| | | 75 | 0.26438 |

It is observed from these figures that the saturation of strain accumulation takes place in the alloy after around 20 cycles under all test conditions.

## 4.6 Post ratcheting tensile behavior

Posts ratcheting tensile tests were carried out on the specimens, which were ratcheted for 100 cycles. The procedure for tensile test is mentioned in Section 3.6. Typical engineering stress-strain graphs obtained from these tests previously ratcheted for $\sigma_a - \sigma_m$ combinations of $\sigma_m = 55$, 65, 75 and $\sigma_a = 25$, 35, 45 are shown in Fig.4.10

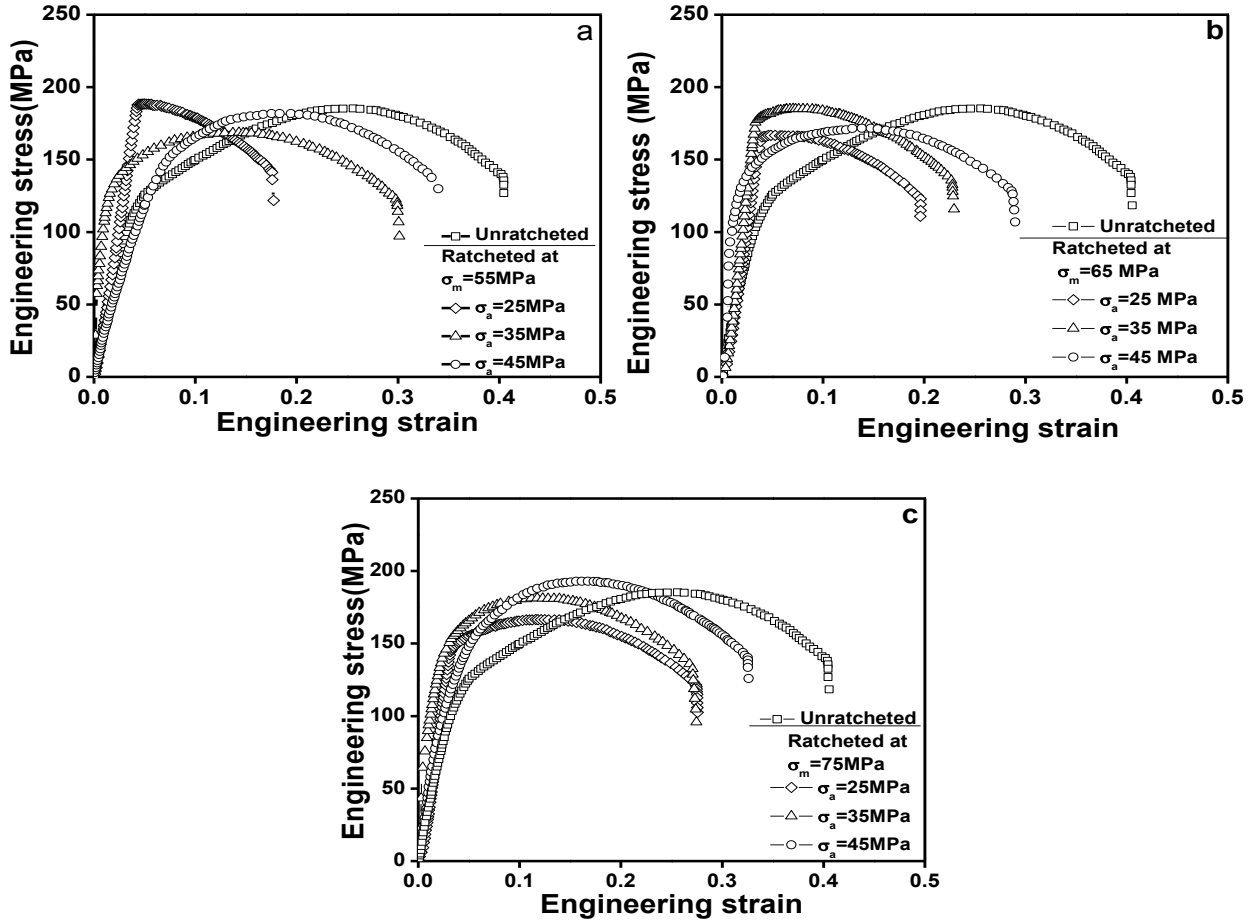


**Fig.4.10:**Typical engineering stress-strain graphs of unratcheted and post ratcheted samples.

It can be observed from Fig.4.10 that the yield strength of the material increase (up to 60%) while the tensile strength marginally decrease (10%). Further, it can be observed from Table 5 that the values of strain hardening exponent and strength coefficient decreased as compared to that of the unratcheted tensile results. The obtained values of yield strength, ultimate tensile strength, percentage uniform elongation and percentage total elongation for these tests as well as for all other tests are given in Table 4.5.

**Table 4.5:** Post ratcheting tensile properties of Aluminum 7075-T6 Alloy

| Material condition | Tensile strength(MPa) | Yield strength(MPa) | $\%\varepsilon_u$ | $\%\varepsilon_l$ | *n* | K (MPa) |
|---|---|---|---|---|---|---|
| Unratcheted | 188 | 70 | 25.58 | 40.297 | 0.3557 | 380 |
| Ratcheted,M55A25 | 185 | 180 | 5.62 | 17.01 | 0.1256 | 283 |
| Ratcheted,M55A35 | 169 | 104 | 14.31 | 3037 | 0.15672 | 264 |
| Ratcheted,M55A45 | 182 | 177 | 20.06 | 33.97 | 0.2170 | 316 |
| Ratcheted,M65A25 | 168 | 166 | 5.55 | 18.33 | 0.1503 | 210 |
| Ratcheted,M65A35 | 185 | 177 | 7.04 | 22.49 | 0.1049 | 263 |
| Ratcheted,M65A45 | 171 | 102 | 14.72 | 29.71 | 0.1684 | 275 |
| Ratcheted,M75A25 | 188 | 100 | 11.94 | 26.56 | 0.1303 | 247 |
| Ratcheted,M75A35 | 167 | 146 | 11.51 | 27.54 | 0.1369 | 273 |
| Ratcheted,M75A45 | 182 | 110 | 17.51 | 31.91 | 0.1727 | 310 |

The strain hardening exponent and strength coefficient values were also estimated for all of these samples and the obtained data are shown in the same table (Table 5). A comparison of all the

results suggests that prior ratcheting test predominantly affects the strength values as well as the strain hardening nature of the material. Earlier investigations on commercial aluminum [58] and Al-6063 alloy [3] suggest that the materials were cyclically hardenable. Few other investigations also suggest that a material can be cyclically hardenable [59] or softenable [28, 29]. However, the material under current investigation shows a mixed nature of hardening – softening feature. Analyses of hysteresis loops generated during cyclic loading suggest that initially the loop area decreases while it increases on further loading. Figure 4.11 shows a comparison among the $2^{nd}$, $50^{th}$ and $100^{th}$ cycles.

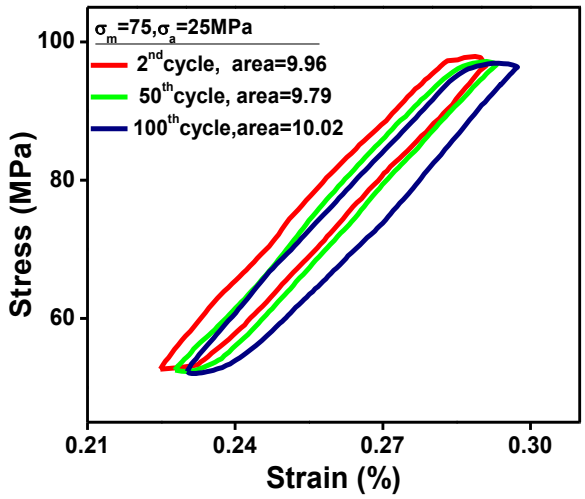


**Fig.4.11:** A typical hysteresis loop of $2^{nd}$, $50^{th}$ and $100^{th}$ cycle at constant mean stress 75MPa and stress amplitude 25 MPa.

The quantitative assessment of loop area also indicates this kind of initial hardening and then softening. The same is seen from the post-ratcheting tensile results of the material. Marginal variation in the tensile strength indicates that due to combined hardening and softening during cyclic loading, the final increment in strength is not up to a high extent.

According to ASM international [49], if the ratio of ultimate tensile strength to yield strength of a material is greater than 1.4 then material is likely to cyclically harden and if it is less than 1.2, then the opposite phenomenon happens. If this ratio is between 1.2 and 1.4, some of the materials may show cyclic hardening, some may show cyclic softening while some remain stable. The material under current investigation shows UTS to YS ratio of 1.02. According to Martin [60] if, 7075 aluminum alloy contains only GP-1 zone kind of precipitates, the material shows cyclic hardening up to 50 cycle and 70-80 cycle its show softening in nature . If the alloy exhibits both GP-1 and θ particles, hardening followed by softening occurs only at (up to 110 cycles) large and intermediate strains. The interpretation is that at high strains, the GP-1 zones are cut sufficiently to disorder the structure and the alloy softens. If the dispersoids present in commercial Al alloys, which are very effective at homogenizing the slip distribution, then it exhibits no softening at any strain level. The current investigation shows that the obtained ratio of ultimate stress to yield stress is in between and presence of GP-1 zone according XRD pattern the alloy behavior as hardening followed by softening nature.

## 4.7 Fractography of post tensile broken specimen

The fracture surface of the broken post tensile specimen was observed under SEM as shown in Fig.4.12. It is evident that the material surface shows only dimples at middle portion and the edges show sheared dimples. Measure of the size of dimples using liner intercept method, according to ASTM standard E-112 [52] is shown in Table 4.6.

**Table 4.6:** Dimple size of unratcheted and ratcheted post ratcheting tensile sample

| Material condition | Unratcheted | M55 A25 | M55 A35 | M55 A45 | M65 A25 | M65 A35 | M65 A45 | M75 A25 | M75 A35 | M75 A45 |
|---|---|---|---|---|---|---|---|---|---|---|
| Dimple size (μm) | 8.44 | 5.02 | 5.51 | 6.92 | 5.61 | 5.89 | 7.43 | 5.85 | 6.23 | 7.85 |

It can be observed from the table that dimple size increases with stress amplitude that is with increasing ratcheting strain. Also one can observe form Fig.4.10 that the engineering strain increase with increasing ratcheting strain; this fact indicates that some of the dimples coalescence and thus the size increases. There are some materials, which exhibit particular zones on the fracture surface. The two fundamental zones of fracture surface were examined, in particular fibrous and shear zone. The radial zone portrayed by spoke- or-star formed cracks and for the most part found to occur at temperature beneath 373K, was not seen at any of the specimens [61]. In the present investigation fibrous and shear zone are observed on the fracture surfaces, the dimples present in the shear zones are elongated in nature, as expected.

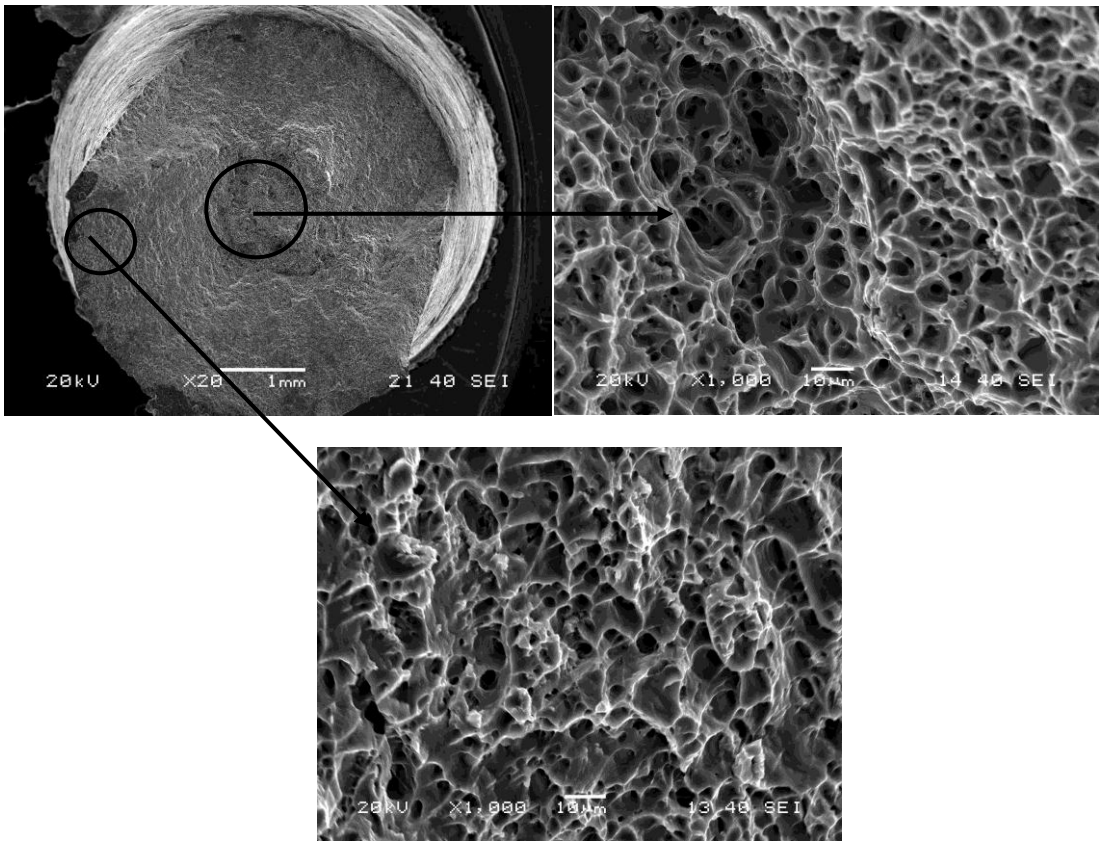


**Fig.4.12 (a):** SEM image of fracture surface at mean stress 55 MPa and stress amplitude 25MPa after post ratcheting tensile tests

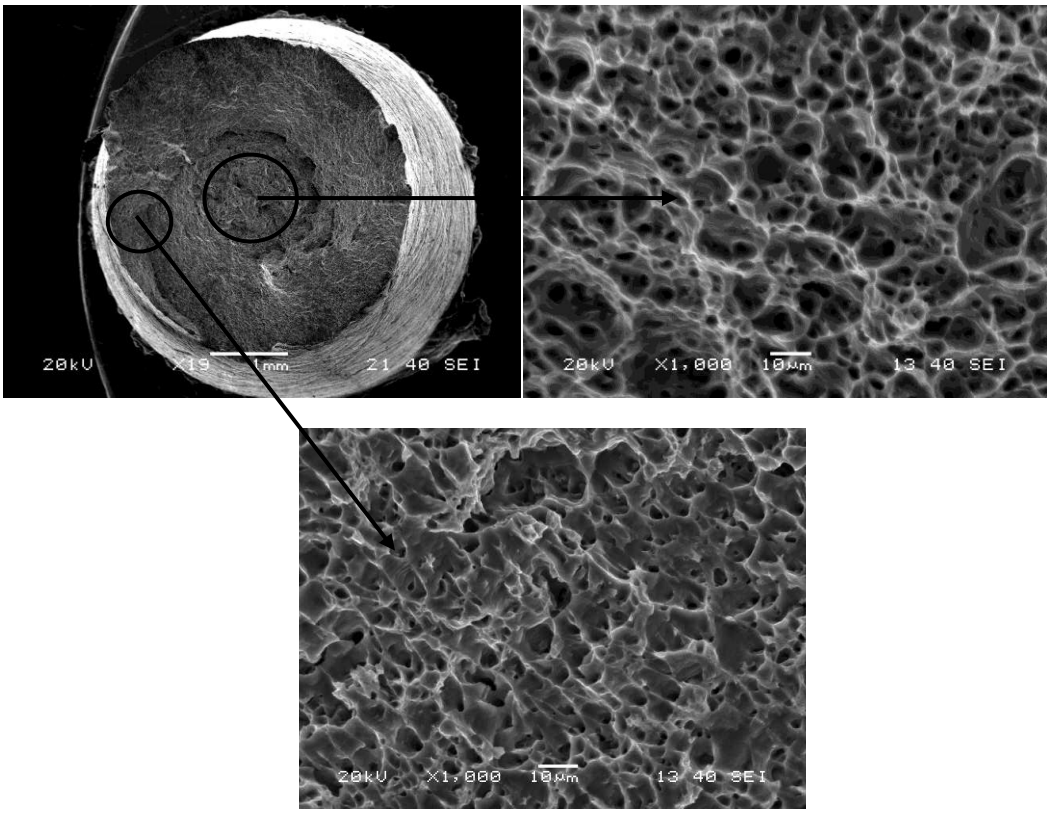


**Fig.4.12 (b):** SEM image of fracture surface at mean stress 55 MPa and stress amplitude 35MPa after post ratcheting tensile test.

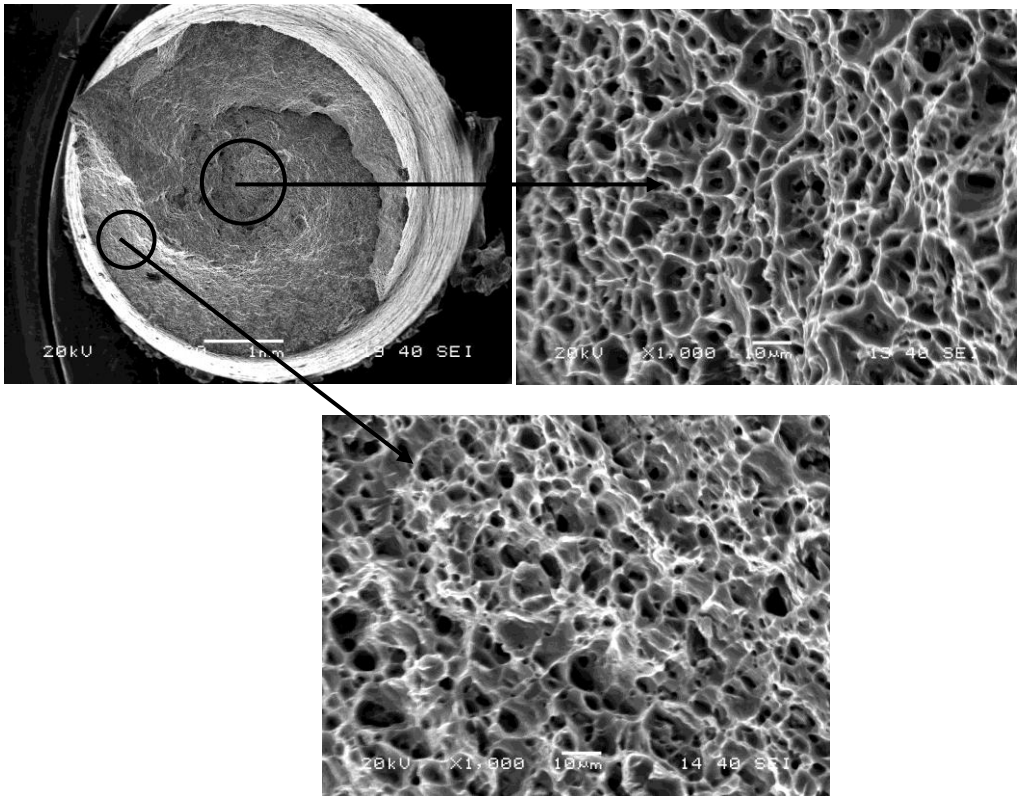


**Fig.4.12 (c):** SEM image of fracture surface at mean stress 55 MPa and stress amplitude 35MPa after post ratcheting tensile test

## 4.8 XRD analysis of tensile and post ratcheting tensile samples

The X-ray diffraction (XRD) analysis were carried out on the investigated aluminium 7075-T6 alloy after tensile and post ratcheting tensile test .The typical XRD pattern obtained are Shown in Fig.4.13.

It can be observed from the XRD pattern that some second phase precipitates $Al_4Cu_9$, $MgZn_2$, $Al_{18}Cr_2Mg_3$ are present in the alloy. It was observed that the peaks were shifting to the lower angle of diffraction (2θ) according to applied mean stress and stress amplitude. The shifting of peaks is generally due to residual stress and lattice distortion [62] in the material.

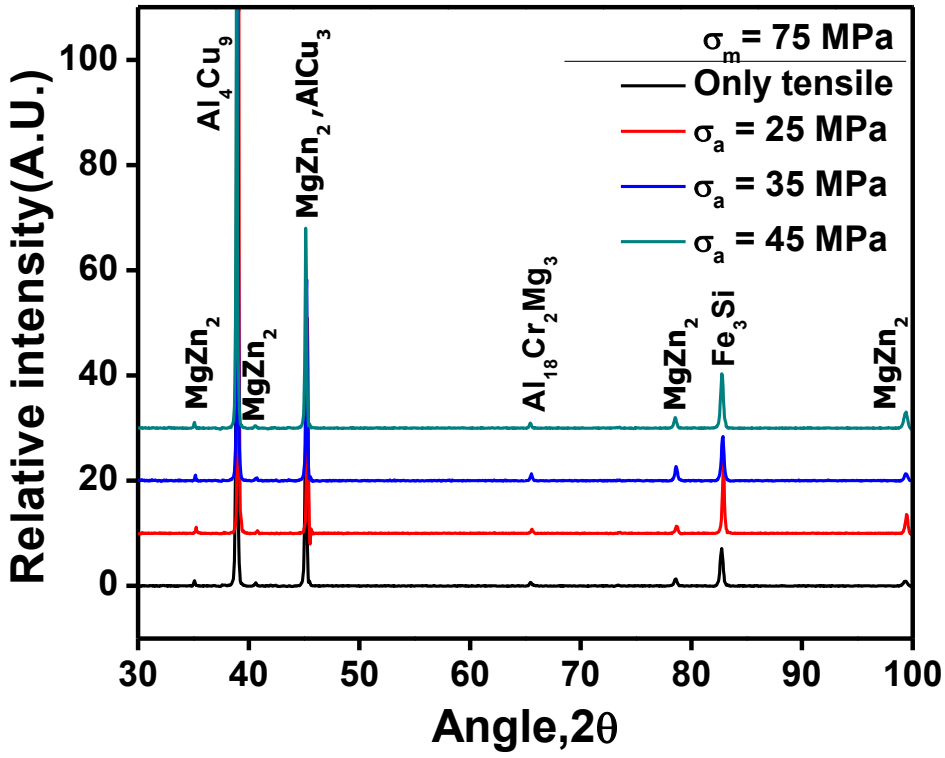


**Fig.4.13:** XRD pattern of aluminum 7075-T6 alloy at different loading conditions.

## 4.9 Summary

In summary, the present investigation has reported the behavior of 7075-T6 aluminium alloy subjected to ratcheting and post ratcheting tensile tests. For different combinations of mean stress and stress amplitudes it is observed that at constant mean stress, by increasing stress amplitude, ratcheting strain increases. The increase in strain accumulation with increasing stress amplitude can be mechanistically expressed with the variations in the heights of the hysteresis loops and thereby corresponding deformation zone.

# Chapter 5

# Conclusions and Scope for future research

# *Conclusions*

## 5.1 Conclusions

The ratcheting fatigue and post-ratcheting tensile tests of aluminum 7075-76 alloy and their pertinent analyses lead to the following major conclusions:

- The strain accumulation due to ratcheting increases with increase in mean stress and/or stress amplitude for either of these is constant. This increase in strain accumulation occurs due to enhanced deformation zone during cycling with higher stress amplitude, which thereby increases the remnant dislocation density.

- The analyses of hysteresis loop generated during cyclic loading indicate that the material exhibits cyclic hardening in the initial fifty cycles. But interestingly, it softens in further cycling up to the range of 70-80 cycles and finally attains a steady state. This feature of softening in the range of 70-80 cycles is attributed to the formation of Al-Cu type precipitates in cyclic loading.

- The post ratcheting tensile results indicate that the yield strength of the material increases whereas the ultimate tensile strength decreases. This is analogous to the observations of hardening followed by softening in cyclic loading.

# *Scope for future research*

## 5.2 Scope for future research

- Study of the ratcheting-fatigue interaction behavior of the alloy.
- Study on effect of other heat treatments such as T4, T5, and T7 etc.
- Ratcheting behavior under tension-compression and negative mean stress condition.
- Multiaxial ratcheting behavior of the investigated alloy.

## References

[1] Smith W., “Principles of materials science and engineering”, New York, McGraw- Hill, 1996.

[2] Altenpohl D. and Kaufman J.G., “Aluminium: technology, applications, and environment”, 6th Edition, Washington D.C: The Aluminium Association 1998.

[3] Dieter G.E., “Mechanical Metallurgy”, SI metric edition, Singapore, McGraw-Hill Book Company, 1987.

[4] Dutta K. and Ray K.K., “Ratcheting phenomenon and post-ratcheting tensile behavior of an aluminium alloy”, Materials Science and Engineering A, vol. 540 (2012), pp. 30–37.

[5] Paul S.K., Sivaprasad S., Dhar S. and Tarafder S., “Cyclic plastic deformation and damage in 304LN stainless steel”, Materials Science and Engineering A, vol. 528 (2011), pp. 4874–4882.

[6] L.Bairstow, The elastic limits of iron and steel under cyclical variations of stress, Philosophical Transaction of Royal Society, vol. 210 (1911), pp. 359–386.

[7] Lazan B.J., “Dynamic creep and rupture properties of temperature-resistant materials under tensile stress”, American Society for Testing of Materials, Proceedings, vol. 49 (1949), pp.757–787.

[8] Kenedy A.J., “Effect of fatigue stresses on creep and recovery”, International Conference on Fatigue of Metals, Institute of Mechanical Engineers, London, (1956), pp. 401–410.

[9] Meleka A. H. and Evershed A. V., “The dependence of creep behavior on the duration of a superimposed fatigue stress”, Journal of Institute of Metallurgists, vol. 88 (1960), pp. 411–414.

[10] Coffin L.F., J.R., “The stability of metals under cyclic plastic strain”, ASME Journal of Basic Engineering, vol. 82 (1960), pp. 671–682.

[11] Benham P.P., “Axial-load and strain-cycling fatigue of copper at low endurance”, Journal of Institute of Metals, vol. 89 (1961), pp. 328–339.

[12] Benham P.P. and Ford H., “Low endurance fatigue of a mild steel and an aluminum alloy”, Journal of Mechanical Engineering and Sciences, vol. 3 (1961), pp. 119–132.

[13] Yang Z. and Wang Z., “Effect of pre strain on cyclic creep behaviour of a high strength spring steel”, Materials Science and Engineering A, vol. 210 (1996), pp. 83–93.

[14] Feaugas X. and Gaudin C., “Ratcheting process in the stainless steel AISI 316L at 300 K: an experimental investigation”, International Journal of Plasticity, vol. 20 (2004), pp. 643–662.

[15] Kawashima F., Ishikawa A. and Asada Y., “Ratcheting deformation of advanced 316 steel under creep–plasticity condition”, Nuclear Engineering and Design, vol. 193 (1999), pp. 327–336.

[16] Gao Q., Kang G.Z. and Yang X.J., “Uniaxial ratcheting of SS304 stainless steel at high temperatures: visco-plastic constitutive model”, Theoretical and Applied Fracture Mechanics, vol. 40 (2003), pp. 105–111.

[17] Chen X., Yu D. and Kim K.S., “Experimental study on ratcheting behaviour of eutectic tin-lead solder under multiaxial loading”, Materials Science Engineering A, vol. 406 (2005), pp. 86–94.

[18] Chen G., Chen X. and Niu C.D., “Uniaxial ratcheting behavior of 63Sn37Pb solder with loading histories and stress rates”, Materials Science and Engineering A, vol. 421 (2006), pp. 238–244.

[19] Jiang Y., Sehitoglu H., “Cyclic ratcheting of 1070 steel under multiaxial stress states”, International Journal of Plasticity, vol. 10 (1994), pp. 579-608.

[20] Gupta C., Chakravartty J. K., Reddy G. R., Banerjee S., “Uniaxial cyclic deformation behaviour of SA 333 Gr 6 piping steel at room temperature”, International Journal of Pressure Vessels and Piping, vol. 82 (2005), pp. 459–469.

[21] Lorenzo F. and Laird C., “Cyclic creep acceleration and retardation in polycrystalline copper tested at ambient temperature”, Acta Metallurgica, vol. 32(5) (1984), pp. 681–692.

[22] Lim C.B., Kim K. S., Seong J. B., "Ratcheting and fatigue behaviour of a copper alloy under uniaxial cyclic loading with mean stress", International journal of fatigue, vol. 31 (2009), pp. 501–507.

[23] Chen X. and Hui S., "Ratcheting behavior of PTFE under cyclic compression", Polymer Testing, vol. 24 (2005), pp. 829–833.

[24] Liu W., Gao Z. and Yue Z., "Steady ratcheting strains accumulation in varying temperature fatigue tests of PMMA", Materials Science and Engineering A, vol. 492 (2008), pp. 102–109.

[25] Kang G., "Uniaxial Time-dependent Ratcheting of SiCp/6061Al Composites at Room and High Temperature", Composites Science and Technology, vol. 66 (2006), pp. 1418–1430.

[26] Yoshida F., "Uniaxial and biaxial creep-ratcheting behaviour of SUS304 stainless steel at room temperature", International Journal of Pressure Vessels & Piping, vol. 44 (1990), pp. 207–223.

[27] Kang G., Gao Q. and Yang X., "Uniaxial cyclic ratcheting and plastic flow properties of SS304 stainless steel at room and elevated temperatures", Mechanics of Materials, vol. 34 (2002), pp. 145–159.

[28] Hassan T., Kyriakides S., "Ratcheting of cyclically hardening and softening materials: I. Uniaxial behaviour", International Journal of Plasticity, vol. 10 (1994), pp. 149–184.

[29] Kang G.Z., Li Y.G., Zhang J., Sun Y.F., Gao Q., "Uniaxial ratcheting and failure behaviours of two steels", Theoretical and Applied Fracture Mechanics, vol. 43 (2005), pp. 199–209.

[30] Wang Y., Yu D., Chen G., Chen X., "Effects of pre-strain on uniaxial ratcheting and fatigue failure of Z2CN18.10 austenitic stainless steel", International Journal of Fatigue, vol. 52 (2013), pp.106–113.

[31] Isobe N., Sukekawa M., Nakayama Y., Date S., Ohtani T., Takahashi Y., Kasahara N., Shibamoto H., Nagashima H., Inoue K., "Clarification of strain limits considering the ratcheting fatigue strength of 316FR steel", Nuclear Engineering and Design, vol. 238 (2008), pp. 347–352.

[32] http://en.wikipedia.org/wiki/Aluminium, Jan 15, 2015.

[33] http://aluminium.matter.org.uk/, Nov 08, 2014.

[34] Feng L. J., Wei P. Z., Xing L.C., Qiang J. Z., Jing C. W., Qiao Z. Z., "Mechanical properties, corrosion behaviors and microstructures of 7075 aluminium alloy with various aging treatments", Trans.Nonferrous Met.Soc.China, vol. 18 (2008), pp. 755–762.

[35] Ellyin F., "Fatigue Damage, Crack Growth and Life Prediction", UK first edition, Chapman & Hall, (1997).

[36] Ringsberg J. W., "Life prediction of rolling contact fatigue crack initiation", International Journal of Fatigue, vol. 23 (2001), pp. 575–586.

[37] Gaudin C. and Feaugas X., "Cyclic creep process in AISI 316L stainless steel in terms of dislocation patterns and internal stresses", Acta Materialia, vol. 52 (2004), pp. 3097–3110.

[38] Lazan B. J., "Dynamic creep and rupture properties of temperature resistant materials under tensile stress", American Society for Testing of Materials, Proceedings, vol. 49 (1949), pp. 757-787.

[39] Manjone M. J., "Effect of pulsating loads on the creep characteristics of aluminum alloy 14S-T", American Society for Testing of Materials, Proceedings, vol. 49 (1949), pp. 788–798.

[40] Ruggles M. B. and Krempl E., The interaction of cyclic hardening and ratcheting for AISI type 304 stainless steel at room temperature-I. Experiments, Journal of Mechanics and Physics of Solids, vol. 38(4) (1990), pp. 575–585.

[41] Xia Z., Kujawski D. and Ellyin F., "Effect of mean stress and ratcheting strain on fatigue life of steel", International Journal of Fatigue, vol. 18 (1996), pp. 335–341.

[42] Van K.D. and Moumni Z., "Evaluation of fatigue-ratcheting damage of a pressurized elbow undergoing damage seismic inputs", Nuclear Engineering Designs, vol. 196 (2000), pp. 41–50.

[43] Tao G. and Xia Z., "Ratcheting behavior of an epoxy polymer and its effect on fatigue life", Polymer Testing, vol. 26 (2007), pp. 451–460.

[44] Kang G., Kan Q., Qian L. and Liu Y., "Ratchetting Deformation of Superelastic and Shape-memory NiTi alloys", Mechanics of Materials, vol. 41 (2009), pp. 139–153.

[45] Dutta K. and Ray K.K., "Ratcheting strain in interstitial free steel", Materials Science and Engineering A, vol. 575 (2013), pp. 127–135.

[46] Dutta K., Sivaprasad S., Tarafder S. and Ray K. K., "Influence of asymmetric cyclic loading on substructure formation and ratcheting fatigue behaviour of AISI 304LN stainless steel", Materials Science and Engineering A, vol. 527 (2010), pp. 7571–7579.

[47] Paul S. K., Sivaprasad S., Dhar S. and Tarafder S., "True stress control asymmetric cyclic plastic behavior in SA333 C–Mn steel", International Journal of Pressure Vessels and Piping, vol. 87 (2010), pp. 440–446.

[48] Bily M., "Cyclic deformation and fatigue of metals" Elsevier Science Ltd., 1993.

[49] Manson S.S. and Halford G. R., "Fatigue and durability of structural materials", ASM International, (2006), pp. 12–15.

[50] Berg L.K., Gjonnes J., Hansen V., Li X. Z., Knutson-wedel, M. Waterloo G., Schryvers D. and Wallenberg L. R., "GP-zones in Al–Zn–Mg alloys and their role in artificial aging", Acta mater. vol. 49 (2001), pp. 3443–3451.

[51] Rao V.V., "An electro method for studying the microstructure and grain size of Al-1.25% Mn alloy", Indian journal of engineering and material science, vol. 11 (2004), pp. 224-226.

[52] E 112-04, "Standard Test Methods for Determining Average Grain Size", Annual Book of ASTM Standards, vol. 03.01 (2004), ASTM, Philadelphia, PA.

[53] E8M-08, "Standard Test Methods for Tension Testing of Metallic Materials", Annual Book of ASTM Standards, vol. 03.01(2008), ASTM, Philadelphia, PA.

[54] E606/E606M, "Standard Test Method for Strain-Controlled Fatigue Testing" ASTM Standards, vol.0.3.01 (2012), ASTM, Philadelphia, PA.

[55] http://asm.matweb.com/, Nov 08, 2014.

[56] Andreatta F., Terryn H., de Wit J.H.W., “Effect of solution heat treatment on galvanic coupling between intermetallics and matrix in AA7075-T6”, Corrosion Science, vol. 45 (2003), pp. 1733–1746.

[57] Kumar P.V., Reddy G.M., Rao K. S., “Microstructure and pitting corrosion of armor grade AA7075 aluminum alloy friction stir weld nugget zone e Effect of post weld heat treatment and addition of boron carbide”, Defence Technology, vol. 20 (2015), pp. 1–8.

[58] Kreethi R., Verma P., Dutta K., “Influence of Heat Treatment on Ratcheting Fatigue Behavior and Post Ratcheting Tensile Properties of Commercial Aluminum”, Trans Indian Inst Met , vol. 68(2) (2015), pp. 229–237.

[59] Tasnim H., Stelios K., “Ratcheting of cyclically hardening and softening materials in uniaxial behaviour”, International Journal of Plasticity, vol. 10 (1994), pp. 149–84.

[60] Martin J.W., “Precipitation hardening: Theory and application”, Woburn, Reed Educational and Professional Publishing Ltd., pp. 156–159.

[61] Kim B. and Shabaik A. H., “High Temperature Properties and Fracture of 4340 alloy Steel”, Fracture, vol. 2 (1977), pp. 19–24,

[62] Cullity B.D., “Elements of X-Ray diffraction”, second edition, Wesley publishing company inc.